CH2018

Klimaszenarien für die Schweiz

gedruckt in der **schweiz**

Klimaneutral
Druckprodukt
ClimatePartner.com/53460-1810-1002

6. Climate extremes and climate indices

Summary

Climate change will modify the frequency, intensity and character of extreme events In the future. This chapter discusses these changes with emphasis given to the long-term climate-change signal (i.e., the forced response), by considering projections for RCP8.5 by the end of the 21st century. However, at the scale of Switzerland, there is substantial decadal and year-to-year variability in extremes, which may dampen or amplify this forced response at timescales of years to decades. Depending on the type of extreme, the forced response will only emerge for a substantial level of anthropogenic warming (i.e. in RCP4.5 and RCP8.5 by the middle to end of the 21st century). The assessment provided in this chapter highlights the following changes in extremes as the most significant:

- More frequent, more intense, and longer-lasting *heatwaves* and *extremely hot days*. Along with central and southern Europe, Switzerland is a hotspot for changes in hot temperature extremes. The anomalous warming of hot extremes is due to increases in the amplitude of natural temperature variations on daily to seasonal timescales. Under RCP8.5, the hottest summer days are projected to warm by 5.4 - 6.1°C in the multi-model median by the end of the 21st century, depending on the region, with a substantial model range (3.9 - 9.4°C) (typical rounded range across models and regions: 4 - 8.5°C; see Chapter 6.4). Changes are substantially lower for RCP4.5 (2.5 - 3.2°C) and RCP2.6 (1.4 - 1.8°C). Likewise, very hot days that currently occur on average on about one day per summer are projected to occur on about 13 - 38 days or during 2 - 5 weeks per summer (typical range across models and regions; see Chapter 6.4).

- More frequent days with *heat stress* (temperature and humidity) and more warm nights as summer temperatures further increase. These changes are largest at low elevations where the population density is typically highest, and heat stress may be further amplified by urban heat island effects. For unmitigated climate change in particular, heat stress is projected to reach levels that have not been observed over the past century in Switzerland. The amplitude of the changes depends on the scenario considered. The number of days with high heat stress increases non-linearly with warming, becoming about 3 - 5 times more frequent for RCP8.5 than for RCP2.6. Under RCP8.5, half of the summer days in low-altitude areas of Ticino might exhibit high heat stress risk by the end of the 21st century (Chapter 6.5).

- Fewer and less intense *cold waves*, *frost days*, and *ice days*. Absolute changes (number of days) are largest at higher elevations and are much more pronounced in the case of non-mitigation scenarios. Given the very high natural internal variability of winter temperatures, cold winter periods will continue to occur for several more decades (Chapter 6.4).

- More frequent and more intense *heavy precipitation events* in all seasons, but particularly in the winter half year. This trend is projected for all event categories, from hourly downpours to multi-day events. The number and intensity of peak events increases much more strongly than mean precipitation, and may increase even in seasons with decreasing mean precipitation. For the RCP8.5 scenario and the end of the century, day-long heavy precipitation events (100-year return levels) are projected to increase by 10 - 25 %, depending on the season and region (multi-model median; Chapter 6.6, Figure 6.21). During the summer season, the projected changes in the intensity of heavy events on daily to hourly time scales are consistent with an increase of 6 - 7 % per degree warming (due to the Clausius-Clapeyron relationship expressing the increase in water holding capacity; Box 6.1). It follows that changes in heavy precipitation intensity increase approximately linearly with the warming and are thus correspondingly smaller for the mitigation scenarios. Confidence in heavy precipitation intensification is now substantially higher, given the evidence from observations and from a new generation of climate models run at unprecedented resolution. However, the EURO-CORDEX simulations still exhibit substantial spread. Along with the warming, there will also be a shift from solid (snow) to liquid (rain) precipitation. The associated intensification of heavy rainfall has implications for the risk of flooding, while the frequency of heavy snowfall events will decrease at low to mid-altitudes (< 2000 m; Chapter 6.6).

- In summer, there is likely a reduction in wet days in RCP8.5 by the end of the century, and the majority of models suggests longer *dry spells* (periods with no rain). Because of the substantial summer warming and the associated increase in evaporative demand, there is likely to be an increase in agricultural droughts (reductions in soil moisture). Relative to temperature and precipitation extremes, the extent of the drying remains rather uncertain (Chapter 6.7).

The RCP8.5 projected changes mentioned above fit into a continental-scale pattern that is in general qualitatively consistent with recent observational trends on a European scale. At the scale of Switzerland, there is significant decadal and year-to-year variability, and a comparison of projected versus observed patterns is difficult.

6.1. Introduction

This chapter covers projections of both climate extremes and climate indices. Here*climate extremes* encompass rare weather and climate events with potentially serious implications for humans, infrastructure, and the environment, whereas *climate indices* describe more frequent events, such as the frequency of warm days (above some absolute threshold, e.g., 25°C). Although these two categories of events are generally very different in terms of impacts, their assessment relies on similar methodologies. Furthermore, there is a smooth transition between the two concepts, depending on the location considered and the threshold employed. For these reasons, these two event categories are addressed in the same chapter. An overview of key climate indicators is provided in Appendix 1.

6.1.1. Extremes in a changing climate

Alterations in the occurrence of extreme events are a key component of climate change. Already the first IPCC Report [163] stated that "changes in the variability of weather and the frequency of extremes will generally have more impact than changes in the mean climate". However, at that time the assessment of extremes in a changing climate mostly relied on conceptual and theoretical considerations, and extreme events featured on only a handful of pages in the 365-page IPCC report. Since then the understanding of extreme events and the ability to simulate extremes has dramatically improved. The most recent IPCC report [168] features extremes on more than one hundred pages, and extremes were also the subject of an IPCC Special Report [167, 311].

The development of Swiss climate scenarios followed a similar pattern. The early climate scenario reports compiled by the Swiss climate research community (e.g., [245]) offered very little quantitative information. Even in the most recent report [56], the information on climate extremes was synthesized predominantly based on a review of the literature; however, for the first time it also included an early analysis of regional climate model (RCM) simulations (see Chapter 8). In comparison, the information provided in the current chapter is more comprehensive, detailed, and quantitative.

Providing quantitative information about extremes is of great practical importance. This is particularly evident in the case of precipitation and runoff events. To date, the dimensioning of critical infrastructure such as bridges, dams, and urban runoff systems has largely been based on observations collected over recent decades. With the advent of climate change, past observational climatologies increasingly lose value as a guide to the future. Consequently, for infrastructure with lifetimes of many decades, new methodologies must be developed that combine the past observational record with climate-change projections.

In principle, extreme events can be defined for any meteorological variable, or any combination of variables. This report gives consideration to the most relevant extremes, including temperature extremes, heat stress (combining aspects of temperature and humidity), precipitation extremes (for hourly, daily, multi-day, and seasonal events), and droughts. In addition, the literature on wind extremes, hail, and thunderstorms is assessed.

6.1.2. Probability of extreme events

The quantitative definition of extreme events is based on the statistical distribution of the variables of interest. This is illustrated in Figure 6.1 using a schematic figure for daily temperature and precipitation events for current and future climatic conditions. The right-hand tail of the distribution represents extremes and can be are defined based on the exceedance of some threshold (colored areas). The figure demonstrates potential changes that may occur with climate change. It is evident that the occurrence of extremes is closely tied to both the center and the width of the distributions, which in the case of temperature are related to its mean and variability, respectively.
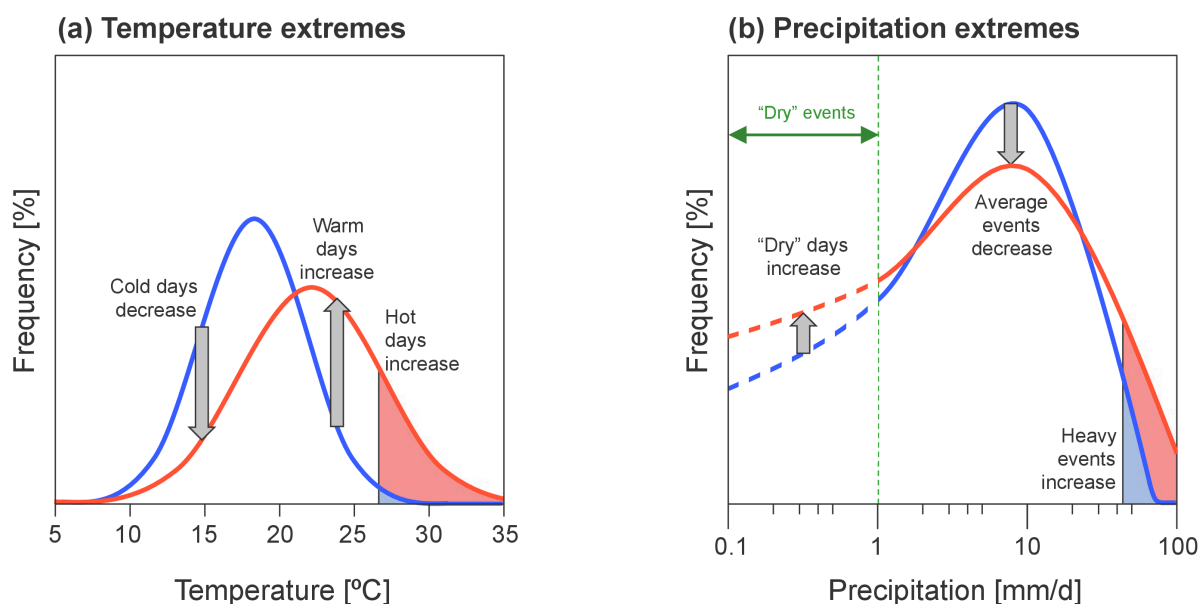
Figure 6.1. Schematic diagram explaining the definition of extreme events for daily (a) temperatures and (b) precipitation using probability density functions (PDFs). Extremes are defined at the tails of the statistical distribution as events exceeding some threshold (colored areas). A shift or change in the distribution with time from the current (blue) to the future (red) distribution leads to changes in the occurrence of extremes. Note that the consideration of precipitation requires the definition of a wet-day threshold (for daily events, usually 1 mm d^{-1}; see the green dashed line in the right-hand panel). The distributions shown are qualitative but are motivated by summer temperatures and precipitation in Zurich. The areas under the PDFs are proportional to the probability of occurrence.

More specifically, the standard deviation of the daily temperature distribution within the summer season typically amounts to 3 - 4 °C. As the expected climate shift is of similar magnitude, associated changes in the probability of hot extremes are very large (compare blue and red areas in Figure 6.1, a). Likewise, because the width of the distribution (which is largely due to natural variations) is large in comparison to the anticipated climate shift, apparent changes in the frequency of extremes may also be caused by chance. Distinguishing natural variations from external (anthropogenic) trends thus represents a challenging task. This difficulty applies to trends in observed (see Chapter 3) as well as simulated climate records (Chapter 6, Chapter 7).

Extreme events may represent a *hazard*, i.e., they have the potential to cause harm, incur damages, or even have catastrophic impacts. However, it is important to note that the definition of "extreme events" utilized in the current report follows a purely statistical concept, using meteorological variables and ignoring potential impacts. The term thus solely represents the hazard component of risk, i.e., the potential of an impact to happen. This is discussed in the next section.

6.1.3. Risk of extreme events

Risks emerge through the interplay of climate- and weather-related hazards, the exposure of goods or people to such hazards, and the specific vulnerability of exposed people, infrastructure, and the environment. Risk can be actively managed, and adaptation allows one to reduce risk, as society shapes exposure and vulnerability. By reducing GHG emissions, one can also indirectly reduce risk, since this

reduces the effect of climate change on the probability of extremes (or hazards).

Risk is the "effect of uncertainty on objectives" [171]. Risk can thus be defined as the combination of the probability of a consequence and its magnitude (i.e., risk = probability x severity). In the simplest case, "x" stands for multiplication, but more generally, it represents a convolution of the respective distributions of probability and severity. According to the IPCC [170], natural hazard risk is the combination and hence a function of hazard, exposure, and vulnerability:

risk = f(hazard, exposure, vulnerability) = probability of hazard x f(intensity of hazard, exposure, vulnerability),

where the last three parameters constitute "severity".

Here, "hazard" describes weather events such as storms, floods, droughts, or heat waves both in terms of the probability of occurrence as well as the physical intensity. "Exposure" denotes the geographical distribution of people, livelihoods, and assets or infrastructure – generally speaking, of all items potentially exposed to hazards, including ecosystems and their services. "Vulnerability" describes how specific exposure will be affected by a specific hazard; that is, it relates the intensity of a given hazard to its impact, such as wind damage to buildings as a function of wind speed or the effect of a flood on a local community and the livelihoods of its residents.

Risk is best measured in the metrics relevant for decision making, e.g., the number of affected people in the context of evacuation, or the replacement value of buildings in the context of property insurance. Risk models therefore attempt to quantify the parameters determining risk in the way most appropriate for the specific purpose. Depending on the purpose, the level of detail in quantification will vary. For a geographical representation, consider, for example, a local flood model at very high resolution (a few decameters) compared to a drought impact model at 10-km resolution. With regard to the vulnerability resolution, consider a general description of building damage due to wind as a simple function of (gust) wind speed, compared to a detailed flood damage function that depends not only on flood height but also on the building construction type, the number of floors, whether or not there is a basement, etc.

Risk management starts with the joint identification of risks and related parameters by all relevant stakeholders, followed by a risk analysis building on the quantification of hazard, exposure, vulnerability, and a careful evaluation of the combination thereof. This analysis forms the basis for the appraisal of specific adaptation options and adaptation planning. Such a comprehensive approach to risk also allows for measurement, reporting and verification of the effectiveness of adaptation, and thus facilitates constant improvements along the risk management cycle.

The present report focuses on the hazard side, i.e., on the frequency and intensity of physical variables describing meteorological events. Consequently, the results presented in this report should by no means be viewed as a quantification of risk. In order to quantify risk, information about exposure and vulnerability would need to be integrated. Nevertheless, the results presented here will serve as a solid basis for risk-based approaches to decision making in the context of weather and climate.

6.2. Methods

6.2.1. Definition of indices and extremes

As indicated in Figure 6.1, the quantitative definition of extreme events and climate indices is based on the statistical distribution of all events of the category under consideration. For temperature, the statistical distribution of daily temperature approximately follows a bell-shaped (Gaussian) distribution (see Figure 6.1, a). If the distribution is shifted toward warmer temperatures (blue and red curves), as expected with climate change, the frequency of cool days will decrease, whereas hot days may become significatnly more common. As illustrated, the statistical distribution may not only shift, but it may change in other aspects as

well. In the current example, it is assumed that it undergoes an increase in variability (or variance), i.e., the distribution widens. Such changes may be more critical than mere shifts in the distribution [163, 179, 306].

For precipitation (see Figure 6.1, b), the situation is more complex. First, precipitation is not Gaussian distributed, and the nature of its distribution strongly depends upon the region and timescale considered (i.e., daily versus hourly precipitation). Second, the description of the precipitation statistics requires the consideration of dry periods. In practice, a wet-day threshold is introduced (e.g., 1 mm d^{-1} for daily events), and events below this threshold are considered "dry". The choice of such a wet-day threshold was originally motivated by observational constraints, as standard rain-gauge instruments suffer from substantial errors at low precipitation intensities. The details of the precipitation distribution below this threshold (dashed lines in Figure 6.1, b) are not further considered.

Although the case of precipitation is far more complex than that of temperature, it is nevertheless evident from Figure 6.1 that their behavior under climate change can be qualitatively comparable: Both distributions are shifted toward the right (i.e., temperature experiences a warming and precipitation an intensification). As a result, the frequency of cold days decreases (warm days increases), and the frequency of small precipitation amounts decreases (heavy events increases).

6.2.2. Extreme and climate indices used in CH2018

One of the major challenges of climate change research is to adequately accounting for all possible changes in statistical distributions. To this end, a number of indices that address different event levels (from frequent, normal events to rare, extreme events) are used. A recommended list of indices is available from a WMO-initiated expert team (Expert Team on Climate Change Detection and Indices, ETCCDI; see [392]). The current report uses a carefully selected list of these indices, but deviates in part from the team's recommendations. In addition, the selection takes into account the recommendations from a user survey [230], which revealed a need for additional information on climate extremes.

The indices considered are best defined using the cumulative distribution function (seeFigure 6.2, b), which expresses the probability that a variable is below (or above) some threshold. There are two classes of indices:

- Frequency indices assess the change in exceedance probability (or exceedance frequency) for a given event size (vertical arrow in Figure 6.2, b). An example of this index is the number of*hot days* (e.g., temperature above 30 °C).

- Intensity indices assess the change in intensity at a given probability level (horizontal arrow in Figure 6.2, b). Percentile indices represent a subset of these indices. For instance, the 99th temperature percentile measures the temperature that on average is exceeded in 1 out of 100 days. Similarly, the 10-year return level of a precipitation event reflects the intensity of a precipitation event that on average occurs once every 10 years.

It is important to note that these two categories of indices are not independent: An increase in one of the measures implies an increase in the other (see Figure 6.2, b). However, relative changes in the two categories are not identical.

(a) Probability distribution

(b) Cumulative distribution
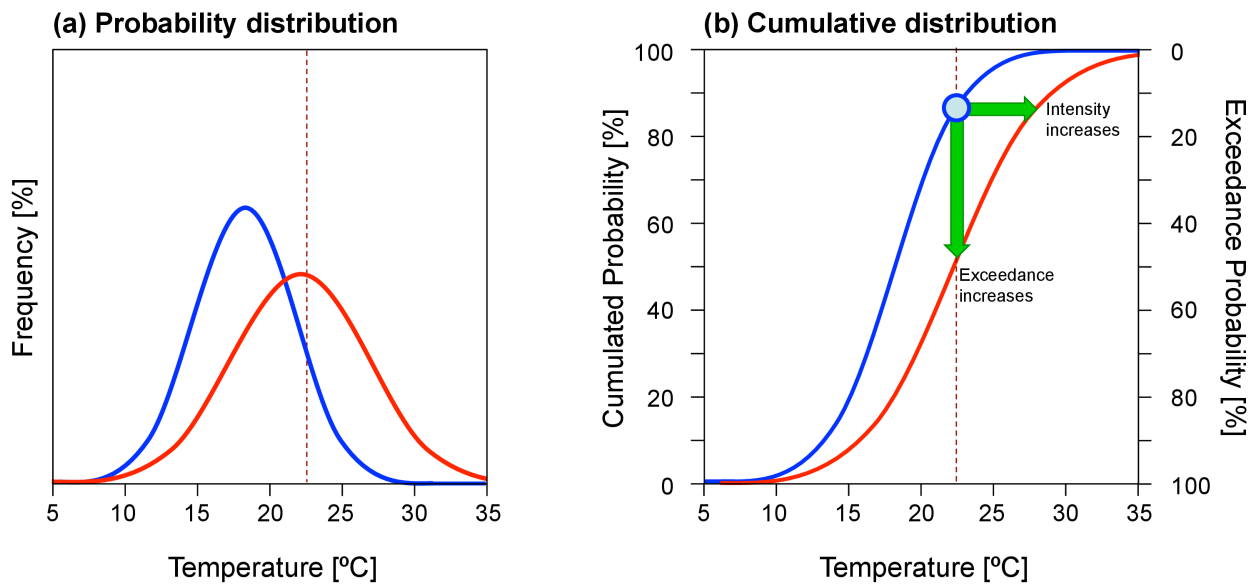
Figure 6.2. Schematic diagram explaining the use of (a) probability density functions (PDFs) and (b) cumulative distribution functions (CDFs) for the analysis of temperature indices and extremes. The CDF can be phrased in terms of the cumulative probability or the exceedance probability (left-hand and right-hand axes, respectively). The green arrows in (b) indicate the two main categories of indices, i.e., frequency indices (measuring the change in exceedance at some fixed intensity) and intensity indices (measuring the change in intensity at some fixed probability).

In the CH2018 project, a large number of different indices have been investigated using observations (Chapter 2) or information from the EURO-CORDEX regional climate models (in this chapter). The indices are summarized in Table 6.1. The optimal choice of an index, as well as the underlying statistical methodology, depends on a number of factors.

Percentile indices are commonly used for temperature and precipitation extremes. These are intensity indices expressing the magnitude of an event that occurs with a given probability. For instance, the 99th percentile of daily temperature refers to temperature events that are exceeded with a probability of 1 %. In the case of daily precipitation, these percentiles may be relative to wet days (within the sample of events with precipitation > 1 mm/day) or relative to all events (wet and dry days). In CH2018, all-day percentiles are used exclusively, as wet-day percentiles are difficult to interpret and may be misleading [305].

Abbreviation	Definition	Unit	Averaging
Temperature extremes			
TXx	Hottest day of the year: Annual maximum of daily Tmax	°C	Annual time-series, 30yr mean
TNn	Coldest night of the year: Annual minimum of daily Tmin	°C	Annual time-series, 30yr mean
TNx	Warmest night of the year: Annual maximum of daily Tmin	°C	Annual time-series, 30yr mean
TXn	Coldest day of the year: Annual minimum of daily Tmax	°C	Annual time-series, 30yr mean
Hot spells			
TXx7d	Hottest week of the year: Maximum 7-day mean of daily Tmax	°C	Annual time-series, 30yr mean
Temperature indices			
TX>25C	Summer days: number of days with Tmax > 25°C	days	Annual time-series, 30yr mean
TX>30C	Hot days: Annual number of days with Tmax > 30°C	days	Annual time-series, 30yr mean
TN>20C	Tropical nights: Annual number of days with Tmin > 20°C	days	Annual time-series, 30yr mean
TN<0C	Frost days: Annual number of days with Tmin < 0°C	days	Annual time-series, 30yr mean
TX<0C	Ice days: Annual number of days with Tmax < 0°C	days	Annual time-series, 30yr mean
Temperature percentiles			
TXp90%	90th percentile of Tmax	°C	Seasonal percentile computed over 30yr
TXp95%	95th percentile of Tmax	°C	Seasonal percentile computed over 30yr
TXp99%	99th percentile of Tmax	°C	Seasonal percentile computed over 30yr
TNp5%	5th percentile of Tmin	°C	Seasonal percentile computed over 30yr
Percentile-temperature exceedances			
TX95P	Hot days: Number of days with Tmax > TXp95% of CTRL	days	Annual time-series, 30yr mean
TX99P	Very hot days: Number of days with Tmax > TXp99% of CTRL	days	Annual time-series, 30yr mean
TN5P	Cold days: Number of days with Tmin < TNp5% of CTRL	days	Annual time-series, 30yr mean
Wet-bulb temperature (based on daily mean temperature and daily mean relative humidity)			
TWx	Maximum of wet-bulb temperature	°C	Annual time-series, 30yr mean
TWg22	Number of days with wet-bulb temperature greater than 22°C	days	Annual time-series, 30yr mean
Precipitation indices			
MEA	Mean daily precipitation	mm/d	Seasonal 30yr mean
FRE	Wet-day frequency: frequency of wet days (R>1mm/day)	fraction	Seasonal 30yr mean
INT	Wet-day intensity: mean precipitation amout on wet days	mm/d	Seasonal 30yr mean
Rx1d	Maximum of 1-day precipitation	mm/d	Seasonal 30yr mean
Rx5d	Maximum of 5-day accumulated precipitation	mm/d	Seasonal 30yr mean
Precipitation Percentiles			
Rp90%	90th all-day percentile of daily precipitation	mm/d	Seasonal percentile computed over 30yr
Rp95%	95th all-day percentile of daily precipitation	mm/d	Seasonal percentile computed over 30yr
Rp99%	99th all-day percentile of daily precipitation	mm/d	Seasonal percentile computed over 30yr
Precipitation return levels for return periods of YY = 5, 10, 20, 50, 100 years (computed using generalized extreme value analysis)			
x1d.YY	YY-year return levels of daily precipitation	mm/d	Seasonal 30yr estimate
x3d.YY	YY-year return levels of 3-day accumulated precipitation	mm/d	Seasonal 30yr estimate
x5d.YY	YY-year return levels of 5-day accumulated precipitation	mm/d	Seasonal 30yr estimate
Drought indices			
CDD	Maximum number of consecutive dry days (R<1mm/day)	days	Seasonal 30yr mean
SPI3	Standardized precipitation index for 3-months acc. precipitation	-	Seasonal 30yr mean
P-E	Precipitation minus evapotranspiration	mm/d	Seasonal 30yr mean
SMA	Standardized soil moisture anomaly	-	Seasonal 30yr mean

Table 6.1. Climate indices and extreme indices used in this study.

The treatment of climate-model biases depends upon the index under consideration. Some of the indices are defined relative to the statistical distribution of the targeted variable; in this case, bias correction is not always needed. This applies, for instance, to changes in percentiles (such as *Tx90%*) and changes in maximum indices (such as *TXx*). However, if an index relies on an absolute threshold (such as the frequency of summer days *TX>25C*), bias correction is usually required. In CH2018, the standard methodology for bias correction is quantile mapping (see Chapter 5). In this chapter, we use bias-corrected data in Chapter 6.3 and Chapter 6.5 and raw model output in the remaining sections. As bias-correction methodologies require an observational reference, the geographical domain that can be considered varies from index to index. For some of the indices, the results can be assessed over the entire computational domain of the models considered (e.g., for changes in annual maximum temperature); for others, a credible observational reference is available for the area of Switzerland (e.g., for the frequency of summer days); and for still others, bias correction is only feasible where surface observations at stations are available (e.g., heat-stress indices). This explains the heterogeneity of the figures in this chapter.

This chapter uses the same ensemble of EURO-CORDEX simulations as considered in Chapter 4. The temporal evolution of the climate-change signal until 2100 can be directly derived from the transient simulations that mostly cover the period 1950 - 2100. In order to incorporate different emission pathways (RCPs), use is made of the time-shift pattern-scaling approach (Chapter 4.2). This approach enables a consistent treatment across scenarios and projection periods.

6.3. Temperature indices

Rising temperatures will have an effect on the frequency of temperature-related indices such as *summer days* and *frost days* [398, 85, 206]. Here, the projected evolution of temperature threshold indices (see Chapter 4.3.2 Definition of indices and extremes) in Switzerland over the course of the 21st century is presented in terms of spatial patterns of the absolute number of days for the individual scenario periods (maps of the respective change signals can be found in Appendix 3.1). In addition, the results of an explicit analysis of the elevation dependency of the indices' changes are described. This exercise is based on bias-corrected model data (multi-model combination) at stations (QM to stations) and on a 2-km high-resolution grid (QM to high-resolution grid; see Figure 5.4).

Due to the absolute nature of the temperature threshold indices considered, they show a strong elevation dependency expressed by large – and in part sharp – elevation gradients (see also Chapter 3.3.2). This is a direct consequence of the elevation dependency of temperature itself and results in high numbers of *summer days* and *hot days* in the lowlands (typically 20 - 60 *summer days* and 0 - 15 *hot days* on the Swiss Plateau and in Alpine valleys in the reference period) and only very few or no occurrences in regions above 1000 m a.s.l. (Figure 6.6). Conversely, the maximum numbers of *frost days* and *ice days* are found in high-Alpine regions (more than 200 *frost days* and more than 150 *ice days* under present-day conditions), whereas only a few *ice days* are observed in the lowlands (Figure 6.6). *Tropical nights* are only found in the low regions and Föhn valleys under present-day conditions. In general, they occur very rarely, namely about once in 1 to 10 years (Figure 6.5 upper row, Figure 13.47 upper row, and Figure 6.6). It should be noted that such low occurrence frequencies are subject to important sampling uncertainties and should be interpreted cautiously. This is true for both the present-day and the future climate.

According to the projections, climate change will have a distinct effect on all indices considered, in particular for the high RCP8.5 forcing scenario and for the period 2085. Most regions are expected to experience increases in the amounts of *summer days*, *hot days*, and *tropical nights*. The latter will also affect large areas of Switzerland where *tropical nights* do not occur in the present-day climate. All regions of Switzerland are projected to face pronounced decreases in the numbers of *frost days* and *ice days*, which is consistent with the observed trend over the past century (see Chapter 3.3.2). *Ice days* will be rare events in the future climates of Ticino and the Lake Geneva region. Projected changes are, in general, less pronounced

for earlier scenario periods and for RCPs 2.6 and 4.5 (see also Appendix 3.1). A summary of the results for each individual index is provided below.

In the reference period, *hot days* (Figure 6.3, Figure 13.49) only occur at low and middle elevations (up to 20 days per year), but a larger proportion of the country will be affected in the future, including considerable parts of the Alps. The frequency of *hot days* is projected to increase by more than 50 days per year in many low-lying regions for the period 2085 of RCP8.5. On the Swiss Plateau, more than 30 hot days per year are expected for the period 2085 and the RCP8.5 forcing scenario; in Ticino and the Lake Geneva region, more than 50 days per year are expected. These numbers are lower for RCP4.5 and especially for RCP2.6 as well as for earlier scenario periods, but are for most parts of the country still higher than for the present-day reference period.

Summer days (Figure 6.5, Figure 13.46, Figure 13.50) occur regularly in most areas under current conditions (up to more than 50 days per year in low-lying regions), except for elevations above 2000 m a.s.l. (see Figure 6.6). In the future, the lowlands are projected to experience many more *summer days*, with up to 100 days per year in low-lying parts of western and southern Switzerland for RCP8.5. Here, frequency increases of more than 50 days per year are possible. Furthermore, the projections suggest the frequent occurrence of *summer days* over large parts of the Alpine area. For the low-emission scenario RCP2.6, frequency increases of typically fewer than 20 days per year are obtained for the period 2085.

Tropical nights (Figure 6.5, Figure 13.47, Figure 13.51) seldom occur under current conditions and are restricted to only a few locations (e.g., to Ticino and very low-lying urban areas; up to about 10 nights per year). Projections suggest an expansion of areas affected by *tropical nights* in the future for all scenario periods and for all forcing scenarios. In the lowlands and in Ticino in particular, *tropical nights* are projected to become frequent events that can occur on average 10 - 30 times per year for the period 2085 and RCP8.5. Exceptions are high-elevation regions above 1500 - 2000 m a.s.l., where *tropical nights* will continue to be rare events even for the most extreme scenario, RCP8.5. For earlier scenario periods and for the RCPs 2.6 and 4.5, the frequency of *tropical nights* typically increases by fewer than 5 events per year.

Frost days (Figure 6.4, Figure 13.52) currently occur regularly in all regions of Switzerland; at high elevations above 2000 m a.s.l., more than 50 % of all days are *frost days* in the present-day climate. Occurrence frequencies at low elevations are considerably smaller (typically fewer than 100 days per year). For all scenario periods, the number of *frost days* is projected to decrease all across Switzerland, with widespread reductions of more than 20 and in part exceeding 80 days per year by the end of the century. For RCP8.5 and the period 2085, low-lying regions are expected to experience very few *frost days*, but typically more than 25 days per year will be obtained for the forcing scenarios RCP2.6 and RCP4.5 and for earlier scenario periods. High elevations in the Alpine region will also experience fewer *frost days*, but frequencies will still exceed 100 days per year for RCP8.5 and the period 2085.

Ice days (Figure 6.5, Figure 13.48, Figure 13.53) are also a common feature of Switzerland's present-day climate and occur at all locations. They are exceptional in Ticino, but they frequently occur in high-Alpine regions, where *ice day* frequencies can exceed 100 days per year. In the future, the number of *ice days* is projected to decrease substantially in all regions, and lowlands will only rarely experience *ice day* conditions. For RCP8.5 and the period 2085, projections suggest an *ice day* fraction of less than 50 % even in high-Alpine regions. This reduction is less pronounced for earlier scenario periods and for RCPs 2.6 and 4.5.

Obs

Reference
Period

Scenario
Periods

RCP2.6   RCP4.5   RCP8.5

2035

2060

2085

Hot Days
(days/year)

60
50
40
30
20
15
10
5
0.1
0

Figure 6.3. Hot days frequency. First row: 2-km observational grid in the reference period 1981 - 2010. Lower rows: Projected ensemble median number (multi-model combination) of the bias-corrected RCM data (QM to high-resolution grid) for the three scenario periods (rows) and the three forcing scenarios (columns). See Figure 13.49 for the respective change signals. Note that the model uncertainty of the change signal is not reflected by the ensemble median number displayed here and can be substantial.
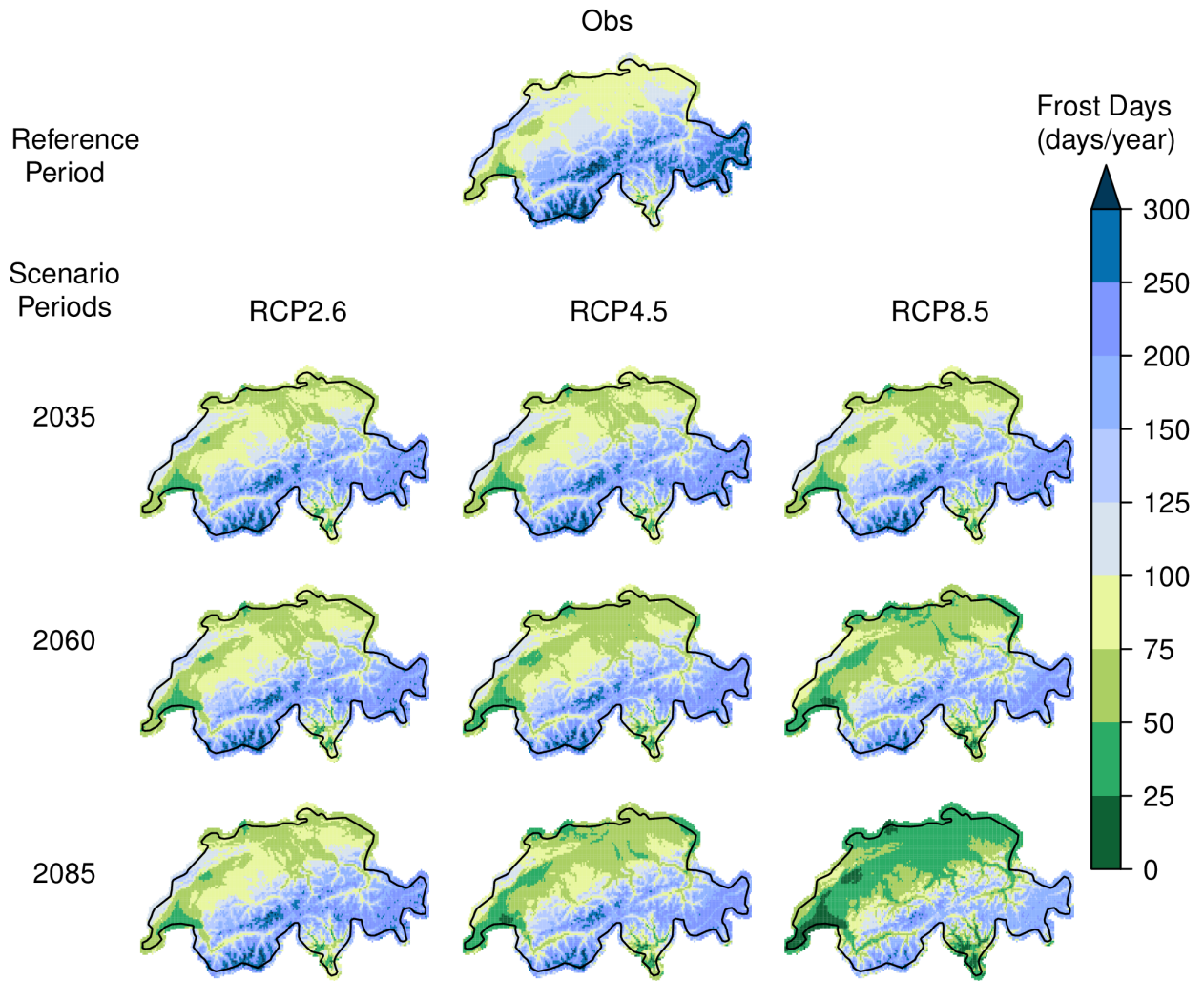
Figure 6.4. As Figure 6.3, but for frost days frequency. See Figure 13.52 for the respective change signals.
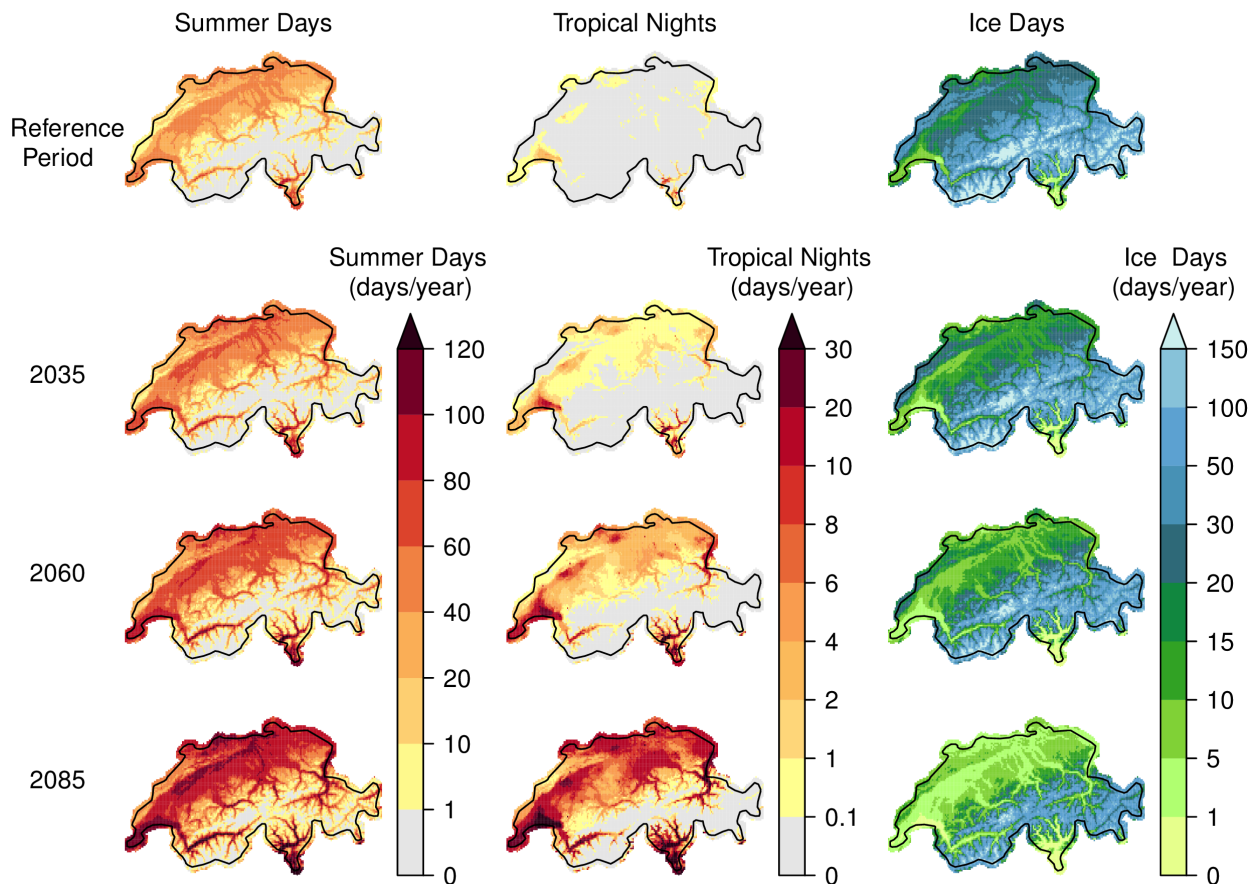
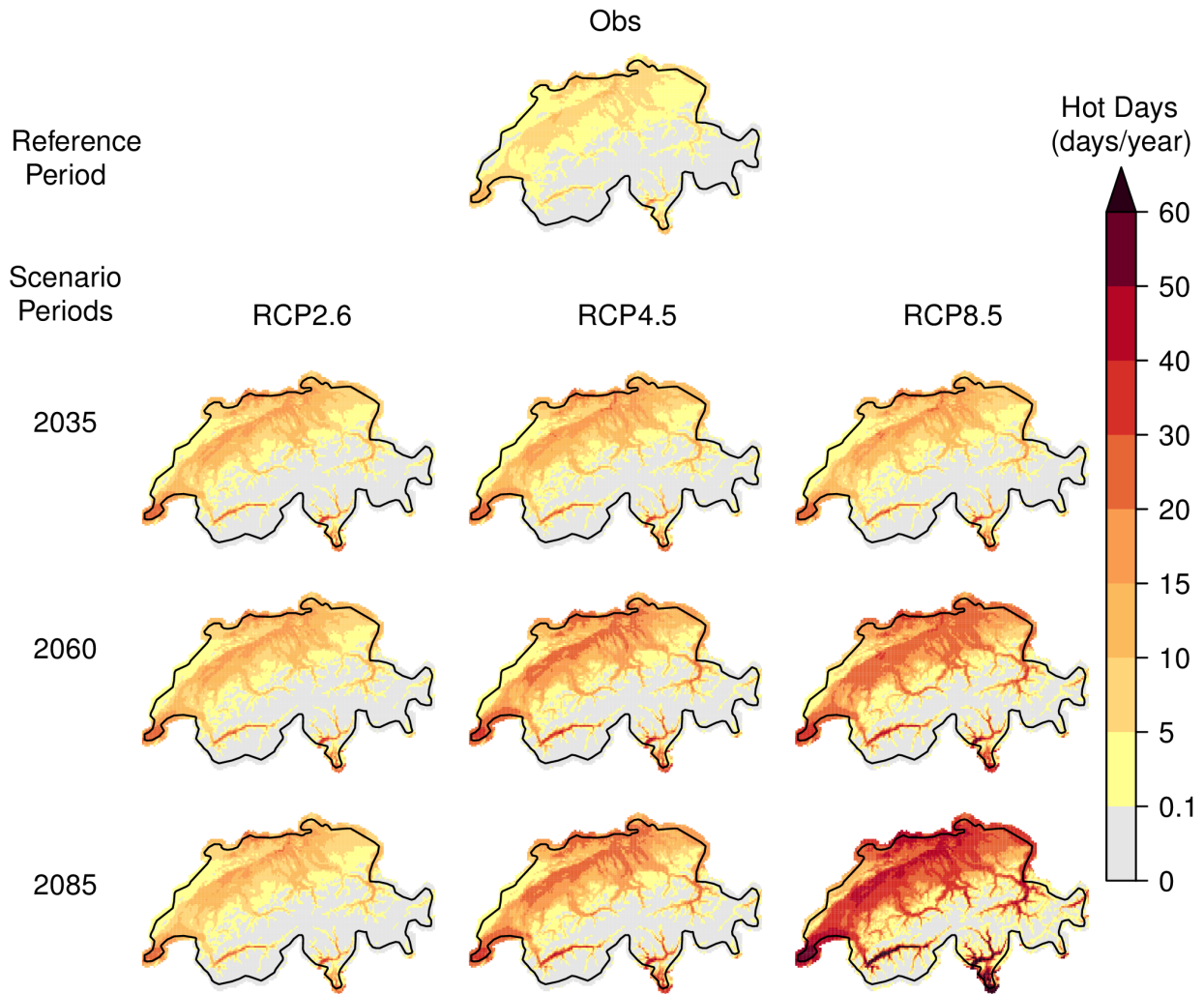*Figure 6.5. Frequency of summer days (left column), tropical nights (middle column), and ice days (right column). First row: 2-km observational grid in the reference period 1981 - 2010. Lower rows: Projected ensemble median number (multi-model combination) of the bias-corrected RCM data (QM to high-resolution grid) for the three scenario periods and for RCP8.5. See Figure 13.46, Figure 13.47, and Figure 13.48 for the full set of forcing scenarios. See Figure 13.50, Figure 13.51, and Figure 13.53 for the respective change signals. Note that the model uncertainty of the change signal is not reflected by the ensemble median number displayed here and can be substantial.*

In summary, both present-day occurrences as well as changes in all temperature indices are subject to considerable *elevation dependencies*. These are visualized in Figure 6.6 and Figure 6.7, which show the absolute value and the change in the respective index as a function of elevation for the period 2085. In general, index regimes are expected to be subject to an upward shift following the general warming. However, even under strong forcing (RCP8.5), high elevations above 2500 m a.s.l. will not experience warm or hot conditions (*summer days*, *hot days*, *tropical nights*) although the temperature on the warmest days will also increase strongly relative to the present-day climatology Chapter 6.4. In contrast, low- and mid-elevation regions below 2000 m a.s.l. are expected to experience drastic increases in indices of hot conditions and might even experience events that do not typically occur in the present-day climate. Examples are the future occurrence of *hot days* and *tropical nights* above 1000 m a.s.l. Cold temperature indices drastically decrease across all elevations. These decreases are, in absolute terms, larger at high elevations but in relative terms still very substantial at low elevations. Under RCP8.5 conditions and by the end of the century, regions below 1000 m a.s.l. might no longer experience *ice days*.
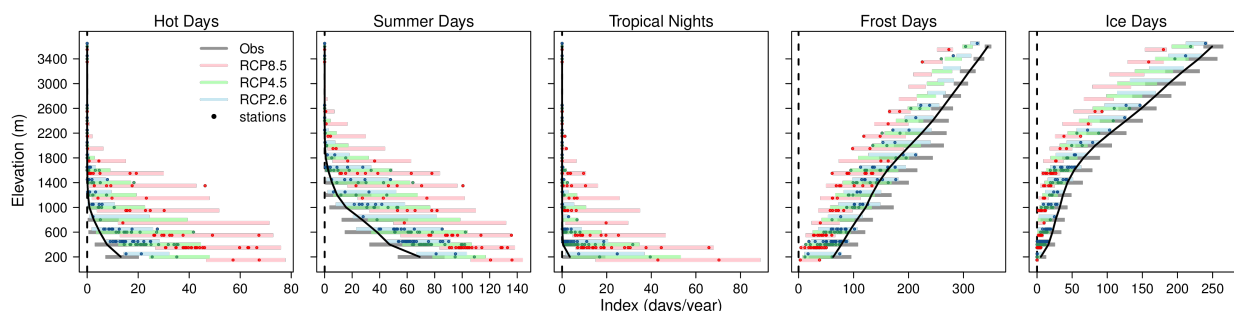
Figure 6.6. Ensemble median frequency (days/year) of the five temperature indices in individual elevation classes (200-m intervals) as represented by bias-corrected data (QM to stations and QM to high-resolution grid; multi-model combination). Black/grey: Observations in the reference period. Color: Bias-corrected data (QM to stations and QM to high-resolution grid) in the late scenario period (2070 - 2099). The points mark the station-based projections (QM to stations; illustrative set); the bars indicate the range of the 2-km observational grid and of the ensemble median of the grid-based QM product (QM to high-resolution grid) in the corresponding elevation class. The black line denotes the elevation-mean number of days in the gridded observations.
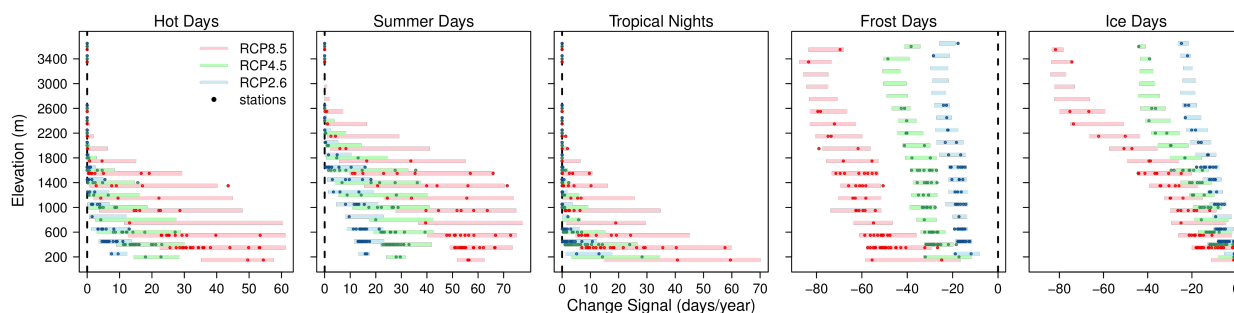

Figure 6.7. Ensemble median change signal (multi-model combination) of the five temperature indices for the late scenario period 2085 and for individual elevation classes (200-m intervals). The points mark the station-based projections (QM to stations; illustrative set); the bars indicate the range of the ensemble median of the 2-km data in the corresponding elevation class.

Finally, turning to the level of individual stations, Figure 6.8, Figure 13.54, and Figure 13.55 present the absolute numbers of the five temperature threshold indices for the reference period and the three scenario periods for the four exemplary sites of Zurich/Fluntern, Weissfluhjoch, Sion, and Lugano. At all four sites, the number of hot events (*hot days, summer days, tropical nights*) increases with time. In Zurich and Sion, *tropical nights* are basically absent in the present-day climate but can reach important occurrence frequencies by the end of the century for RCP8.5 (about 10 to 20 nights per year for the multi-model ensemble median; Figure 6.8). In Lugano, frequencies of about 10 nights per year already occur today. For RCP8.5, this number might increase to between 60 and 90 nights per year (taking into account model uncertainty) by the end of the century – more than every other summer night. Weissfluhjoch does not experience hot extremes in the present, and even for RCP8.5 future occurrences are only obtained for a few model chains but typically not for the multi-model ensemble median. Conversely, cold extremes are projected to decrease at all sites. For RCP8.5, Lugano might no longer experience any *ice days* at all by 2085.
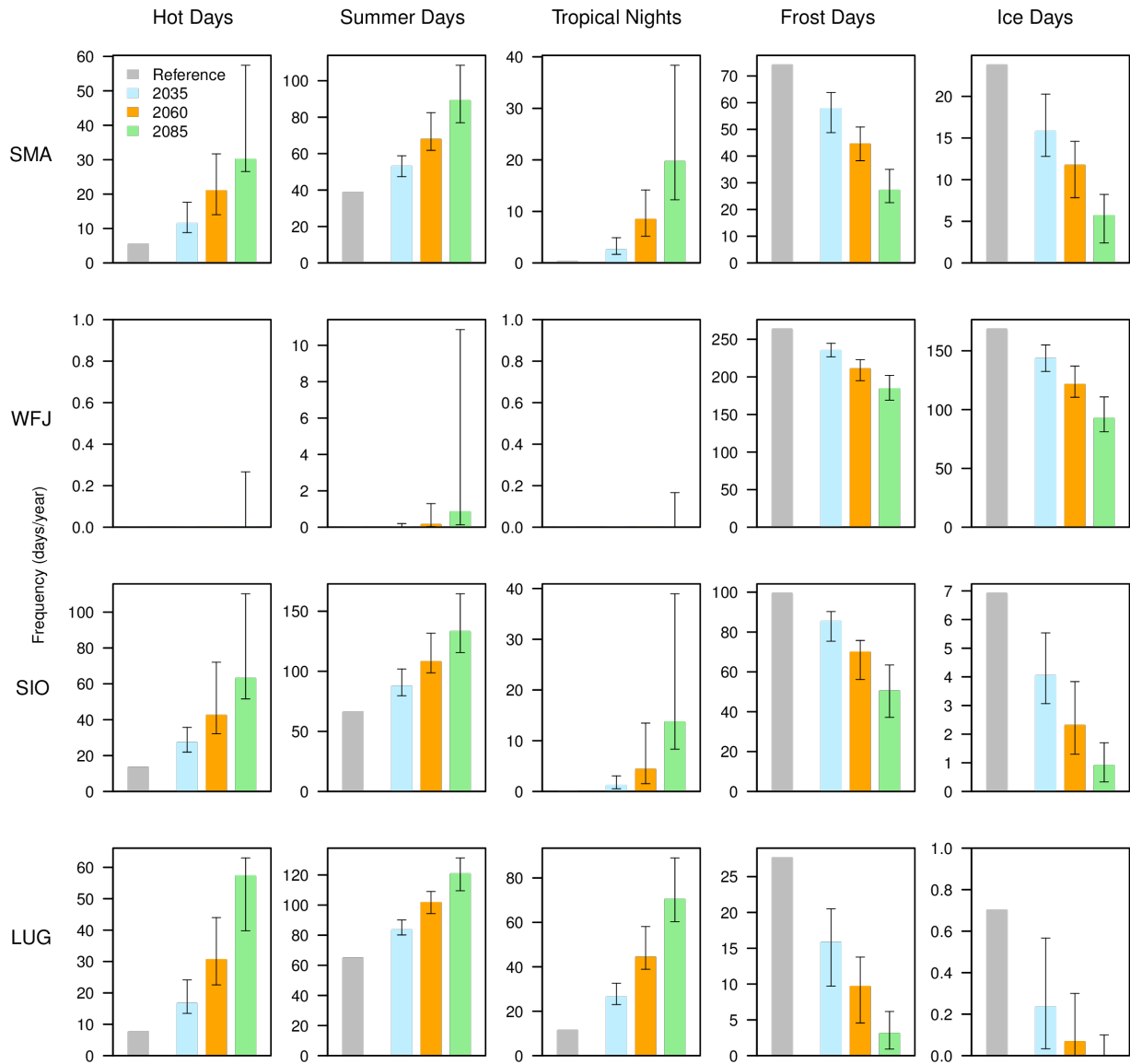
Figure 6.8. Frequency of hot days, summer days, tropical nights, frost days, and ice days in the reference period (observations) and in the three scenario periods (multi-model combination; QM to stations) for RCP8.5 at the four exemplary sites of Zurich/Fluntern (SMA), Weissfluhjoch (WFJ), Sion (SIO), and Lugano (LUG). Bars indicate the ensemble median number; whiskers, the 5 - 95 % model range. See Figure 13.54 and Figure 13.55 for RCP2.6 and RCP4.5.

6.4. Temperature extremes

6.4.1. Heat extremes

Along with increasing summer mean temperatures, hot extremes are virtually certain to increase [66, 311] and become more frequent, intense, and persistent across all land regions globally. Likewise, over Switzerland, heat extremes (here expressed as the maximum temperature of the *hottest day of the year TXx*) are projected to intensify. Depending on the region, the best estimate (multi-model median) for the intensification corresponds to 1.8 - 1.9 °C by 2035, 3.4 - 3.6 °C by 2060, and 5.4 - 6.1 °C by 2085 (Figure 6.10) in RCP8.5, depending on the region. Best estimates for changes are much smaller for RCP4.5 (2.5 - 3.2 °C) and RCP2.6 (1.4 - 1.8 °C). Note that these best estimates include very large uncertainties due to structural and parametric model uncertainties and internal variability. For example, projected *TXx* changes by 2085 for RCP8.5 vary between 3.9 °C and 9.4 °C, depending on the model (typical rounded range across Switzerland 4 - 8.5 °C). The *TXx* changes are consistent with the warming of the *warmest night of the year TNx* (Figure 13.56) and the *hottest week of the year TXx7d* (Figure 13.58), which is a measure of heatwave intensity. The intensification of the *hottest day of the year TXx* (Figure 6.9) is projected to substantially exceed the corresponding summer mean warming (Figure 6.11), an amplification that is consistent with the rest of south-central Europe. This amplification of heat extremes results from enhanced interannual to day-to-day temperature variability and increasing diurnal temperature ranges (Figure 6.11), which is in accordance with earlier generations of regional and global climate models [306, 313, 110, 103, 108, 249, 54]. It has been suggested that the increase in the variability of summer temperatures and in the diurnal temperature range is related to land-atmosphere interactions, including the altered partitioning of sensible and latent heat flux as a result of drying vegetation as well as reduced cloud cover and atmospheric relative humidity [313, 110, 54]. Although the temperature variability increase is robust across models, there is not yet clear observational evidence (Chapter 4.4) [77, 324, 298]. In the European context, the intensification of hot extremes is most pronounced north of the Mediterranean Sea, including France and Switzerland (Figure 6.9). Switzerland thereby forms part of a hotspot region that has experienced one of the strongest intensifications of heat extremes over recent decades [82, 106]; moreover, this region is projected to be one of the areas that will experience the strongest future intensification of hot extremes worldwide [249, 104, 312]. Although the sign of the change is robust (warming), these projections exhibit a large model spread (Figure 6.10) due to uncertainty in the regional mean warming (see section) and due to factors specifically amplifying or damping variability and extremes, such as potential circulation changes [68, 159], land surface feedbacks [358, 356, 110, 359], aerosol forcing [323], and irrigation and land-use changes [73, 341, 155].
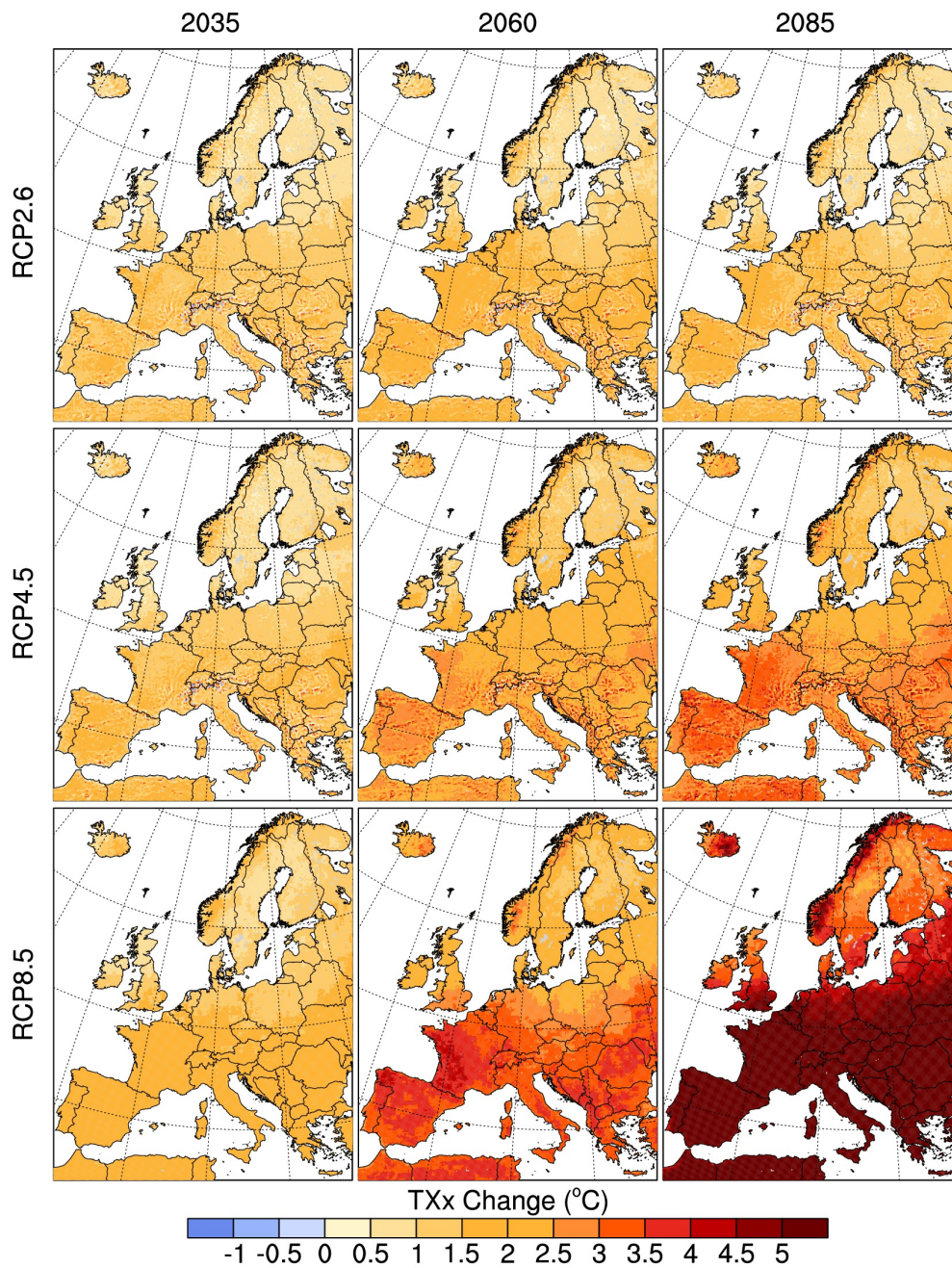
Figure 6.9. Multi-model median change in hot extremes (TXx) by 2035, 2060, and 2085 in RCP2.6, RCP4.5, and RCP8.5 with respect to present-day conditions (°C).
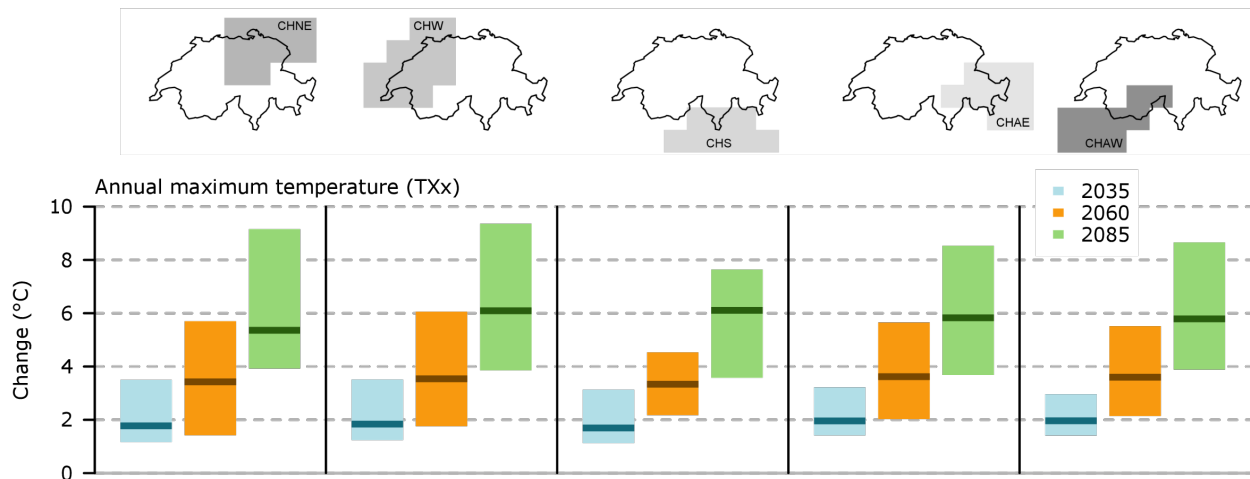
Figure 6.10. Change in hot extremes (TXx) (°C) by 2035, 2060, and 2085 (RCP8.5) averaged across five regions in Switzerland with respect to present-day conditions.
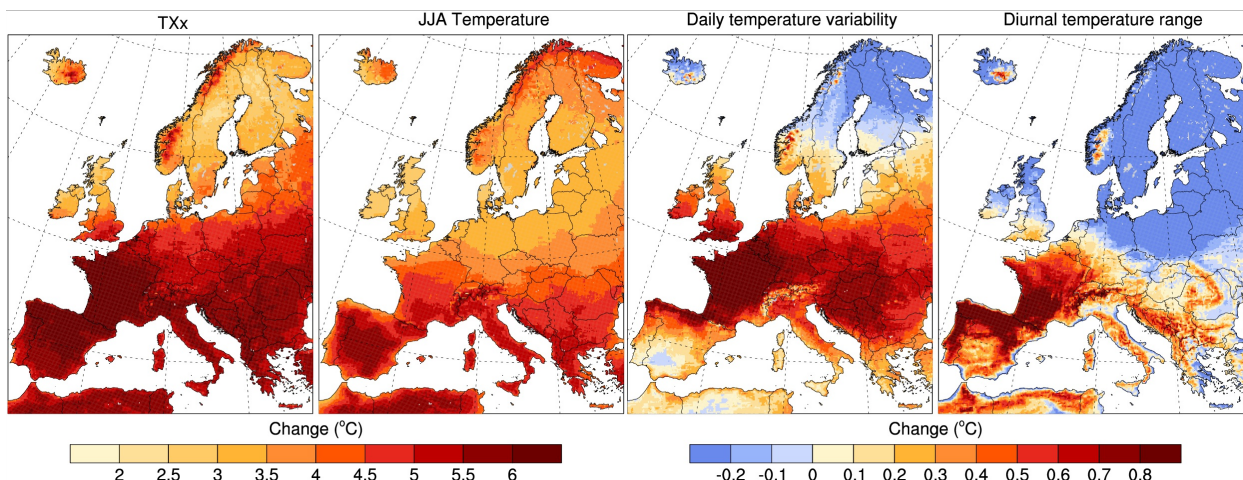

Figure 6.11. Multi-model median change in hot extremes (TXx), summer mean temperature, daily summer temperature variability (standard deviation of daily temperature in summer), and diurnal temperature range (DTR) by 2085 in (RCP8.5) with respect to present-day conditions (°C).

Heat extremes are expected to become not only more intense but also more frequent. The number of *very hot days* (*TX99P*, today expected to occur on about 1 day per summer) is projected to increase in the multi-model median to 2 - 4 days by 2035, 6 - 11 days by 2060, and 13 - 23 days in RCP8.5, depending on the region ([Figure 6.13](#)) (typical rounded model range across Switzerland 4 - 18 days by 2060 and 13 - 38 days by 2085 in RCP8.5). Consequently, such *very hot days* are expected to occur during about 2 - 5 weeks per summer season by 2085 rather than on one day per summer today. The increase in the number of *very hot days* is greater over southern Switzerland; this is consistent with the north-south warming gradient over Europe projected to lead to the strongest regional increase in very hot days over southern Europe ([Figure 6.12](#)). Likewise, this north-south gradient is consistent with the pattern of *hot days* (*TX95P*) ([Figure 13.59](#)) and previous multi-model experiments showing the strongest increase in *very hot days* over the areas of strongest summer warming [103, 11]. *Very hot days* often occur as a cluster of consecutive days, referred to as a heatwave. Models consistently project more frequent, more intense, and longer-lasting heatwaves over Switzerland [25, 103, 249, 60, 285, 322].
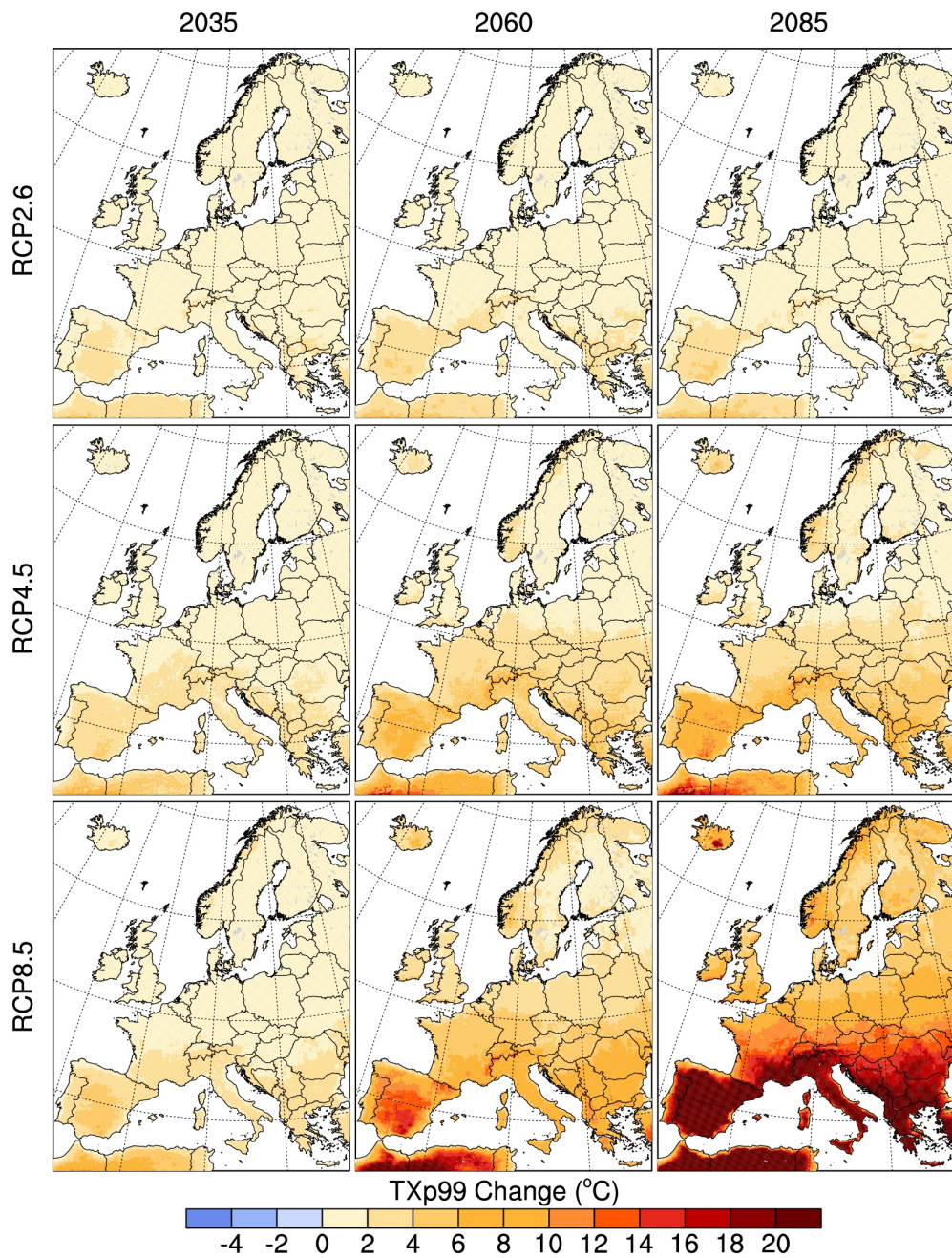
Figure 6.12. Multi-model median change in the number of very hot days (TX99P) by 2035, 2060, and 2085 in RCP2.6, RCP4.5, and RCP8.5 with respect to present-day conditions (days).
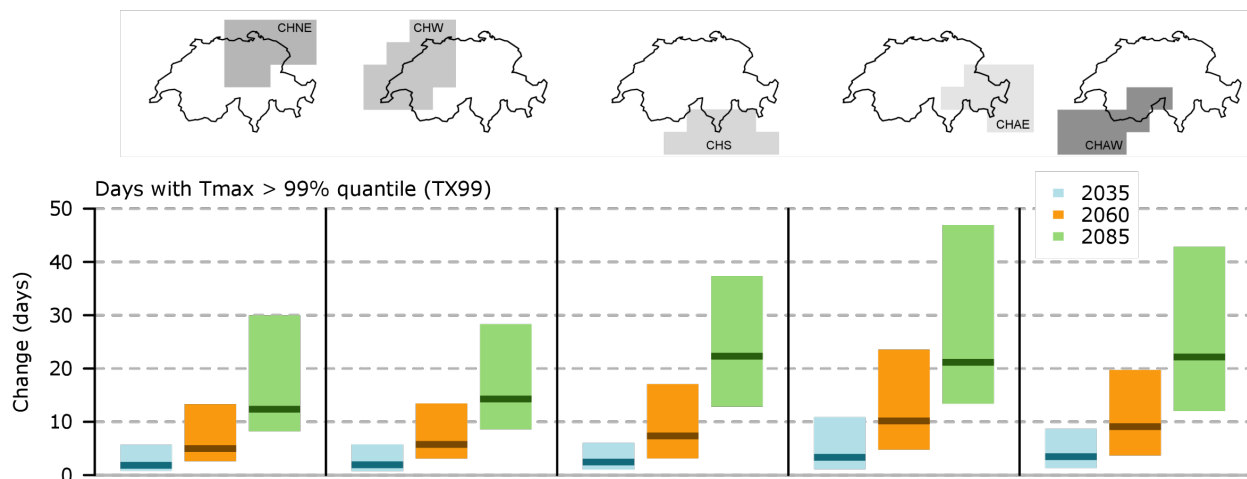
Figure 6.13. Change in the number of very hot days (TX99P (days)) by 2035, 2060, and 2085 (RCP8.5) averaged across five regions in Switzerland with respect to present-day conditions.

6.4.2. Cold extremes

Cold extremes, in contrast to hot extremes, are projected to become less intense and less frequent with warming winter temperatures. Cold extremes in Switzerland (here expressed as *TNn*, the minimum temperature of the *coldest night of the year*) are projected to warm in the multi-model median by 2.0 - 2.3 °C by 2035, by 4.1 - 4.4 °C by 2060, and by 6.2 - 6.9 °C by 2085, depending on the region (Figure 6.15). Changes by 2085 are much smaller for RCP4.5 (3.7 - 4.1°C) and RCP2.6 (2.2 - 2.9 °C). For all best estimates, the model uncertainty is very large, amounting to 3.5 - 11.3 °C for RCP8.5 by 2085. Notably, a substantial fraction of this large uncertainty is related to internal variability [102]. Cold extremes are projected to warm substantially more than the corresponding mean winter temperatures (Figure 6.16), which is consistent with previous regional and global multi-model projections [76, 108, 249]. This amplified warming results from a reduction in the day-to-day winter temperature variability arising from snow-albedo feedbacks [109] and from the relatively strong warming in the source regions of cold-air advection (the continental high-latitudes) due to Arctic amplification and land-sea contrast [76, 308, 158]. Consistent with the north-south warming gradient across Europe (Figure 6.14), cold extremes are projected to warm somewhat more in northern than southern Switzerland. Additionally, very cold days are projected to become less frequent, and cold waves to become shorter. However, given the very high variability of winter temperatures and cold extremes in particular, cold extremes are expected to sporadically occur for several more decades.
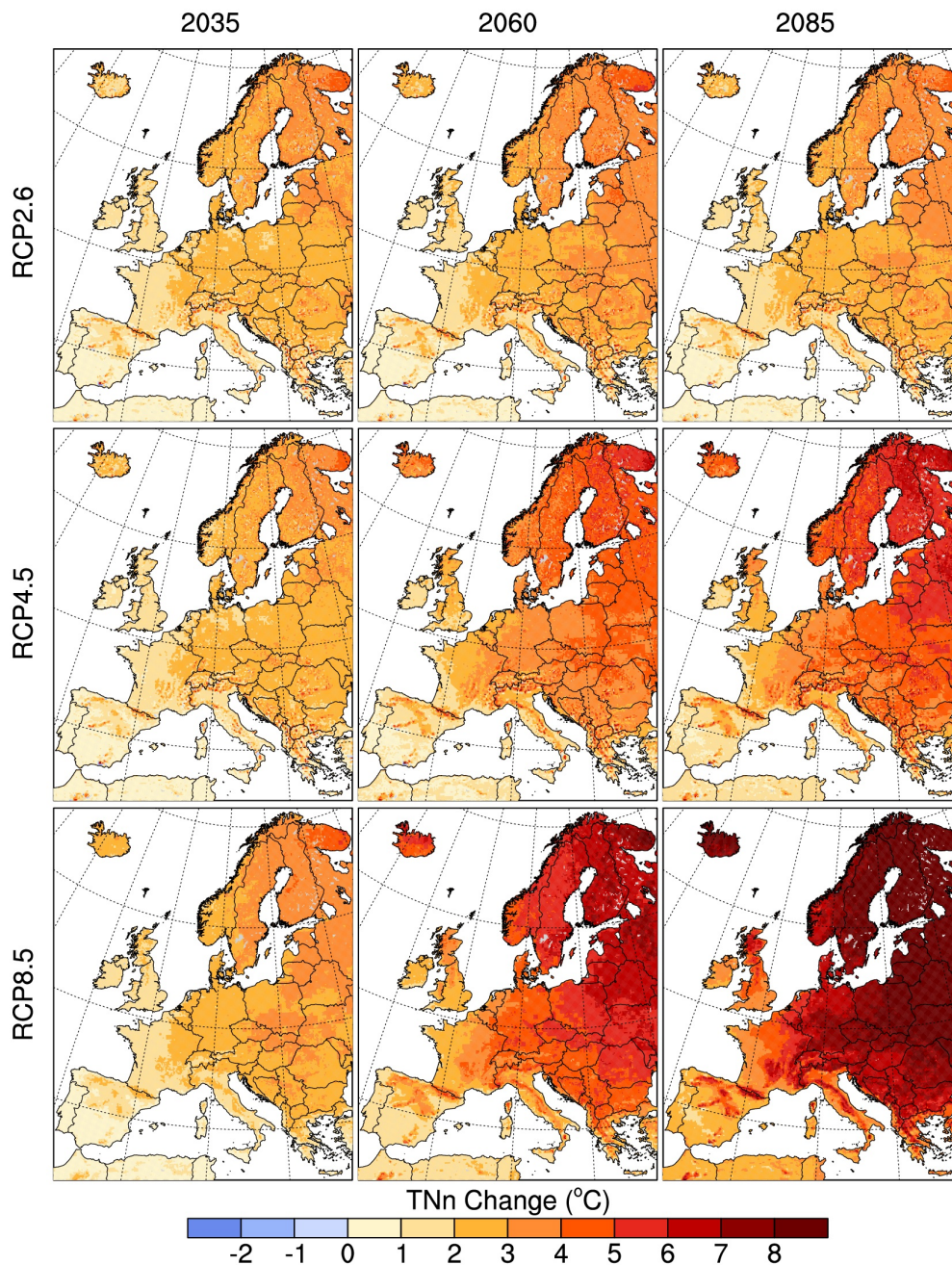
Figure 6.14. Multi-model median change in cold extremes (TNn) by 2035, 2060, and 2085 in RCP2.6, RCP4.5, and RCP8.5 with respect to present-day conditions (°C).
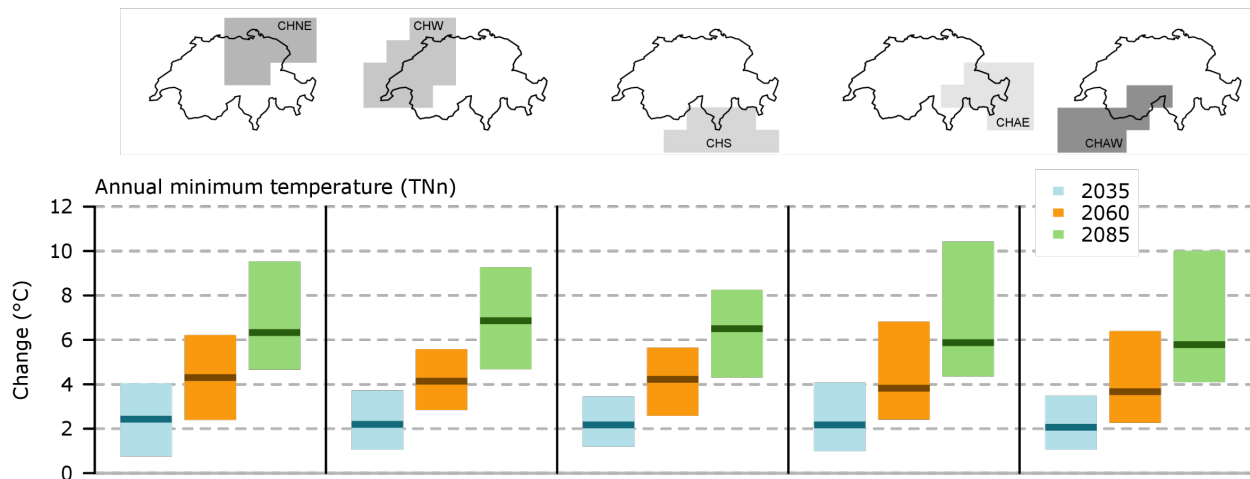
Figure 6.15. Change in cold extremes (TNn) (°C) by 2035, 2060, and 2085 (RCP8.5) averaged across five regions in Switzerland with respect to present-day conditions.
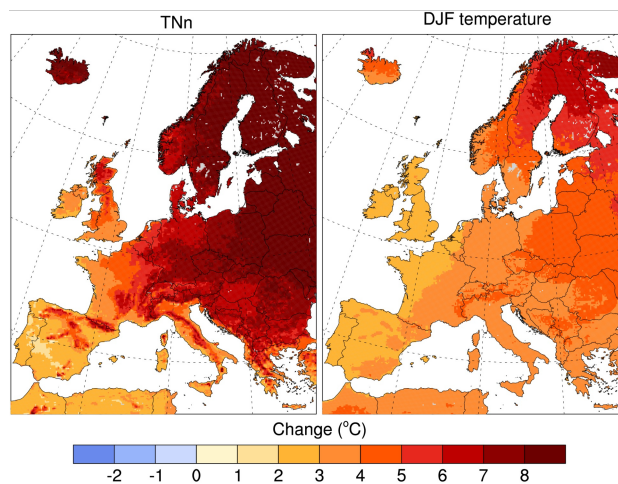
Figure 6.16. Multi-model median change in cold extremes (TNn) and in winter mean temperature by 2085 in (RCP8.5) with respect to present-day conditions (°C).

6.5. Heat stress

An extreme situation can result from a combination of several variables (multivariate extremes; e.g., [4]). This is the case for heat stress, which depends not only on temperature but also on humidity [105]. As explained in Chapter 3.2.1, the wet bulb temperature (TW), based on daily maximum temperature and daily mean specific humidity, is used here to assess heat stress.

The temporal evolution of seasonal maximum wet bulb temperature indicates a continuous increase until the end of the century (Figure 6.17). In the past, in Zurich, Geneva, and Sion, the threshold of 22 °C was only exceeded in extreme summers (e.g., 2003, 2010; black lines), but projected values in these locations are well above that threshold from mid-century onward for RCP8.5.
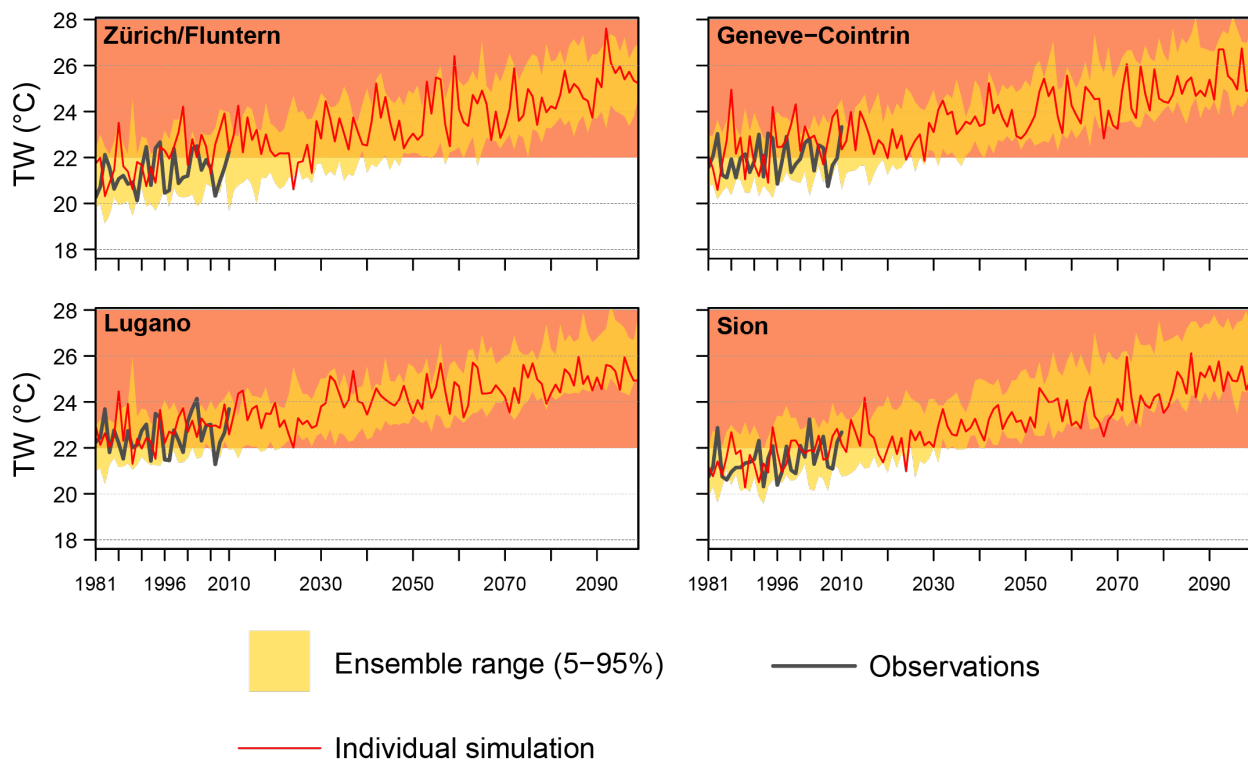
Figure 6.17. Temporal evolution of the summer maximum wet bulb temperature (°C) at four Swiss stations for RCP8.5. The maximum value for each summer is obtained from the maximum daily heat stress values smoothed with a 3-day moving average. Observed values are depicted by the black line, the shading indicates 90 % of the model range, and the red line illustrates an individual simulation (MPI-M-MPI-ESM-LR CLMcom-CCLM4-8-17 for EUR11) as an example.

TW-derived indices are projected to gradually increase over the course of the century at all stations (Figure 6.18). Under scenario RCP8.5, the maximum wet bulb temperature *TWx* increases by 1 - 2 °C, 2 - 3.5 °C, and 3 - 4.5 °C (multi-model median, depending upon the station) in the three scenario periods, respectively. For instance, in Lugano, summer mean and maximum TW are projected to reach 21 - 23 °C and 25 - 27 °C, respectively, in the late 21st century. Heat stress extremes, unlike temperature extremes, show an increase in the upper tail of the distribution similar to the increase in the mean. This absence of amplification of the climate-change signal may be caused by the role of humidity in the TW, since the slight decrease in relative humidity (Figure 13.39) might counteract the larger increase in extreme temperatures. The projected number of summer days with TW >22 °C (*TWg22*) suggests that, on average, more than one-third of summer days will feature severe heat-stress-prone conditions in many locations on the Swiss Plateau (Zurich, Basel, Geneva) and Alpine valleys (Sion, Interlaken, Chur). Ticino is the region with the largest increases in *TWg22*, with increments of up to 15, 30, and 45 days in the three scenario periods, respectively. In mountainous stations, *TWg22* only slightly increases or does not change, since the threshold of 22 °C is hardly ever exceeded (0 - 2 days). These results for *TWg22* are consistent with the findings of [398] for summer days in Switzerland.

Similar regional patterns are found for RCP2.6 and RCP4.5 until mid-century (Figure 13.60, Figure 13.61), also with the largest increases in heat stress indices in Ticino and stations in the lowlands. For RCP2.6, the projected values in the late 21st century scarcely differ from the mid-century values, reaching 19 - 20 °C and 23 - 24 °C for mean and maximum TW in Lugano, respectively. Summer mean and maximum TW are projected to reach 20 - 21 °C and 24 - 25 °C in the late 21st century for RCP4.5. *TWg22* differs substantially between RCP2.6 and RCP8.5 in magnitude and spatial extent, with such summer days about 3 - 5 times more frequent for RCP8.5.
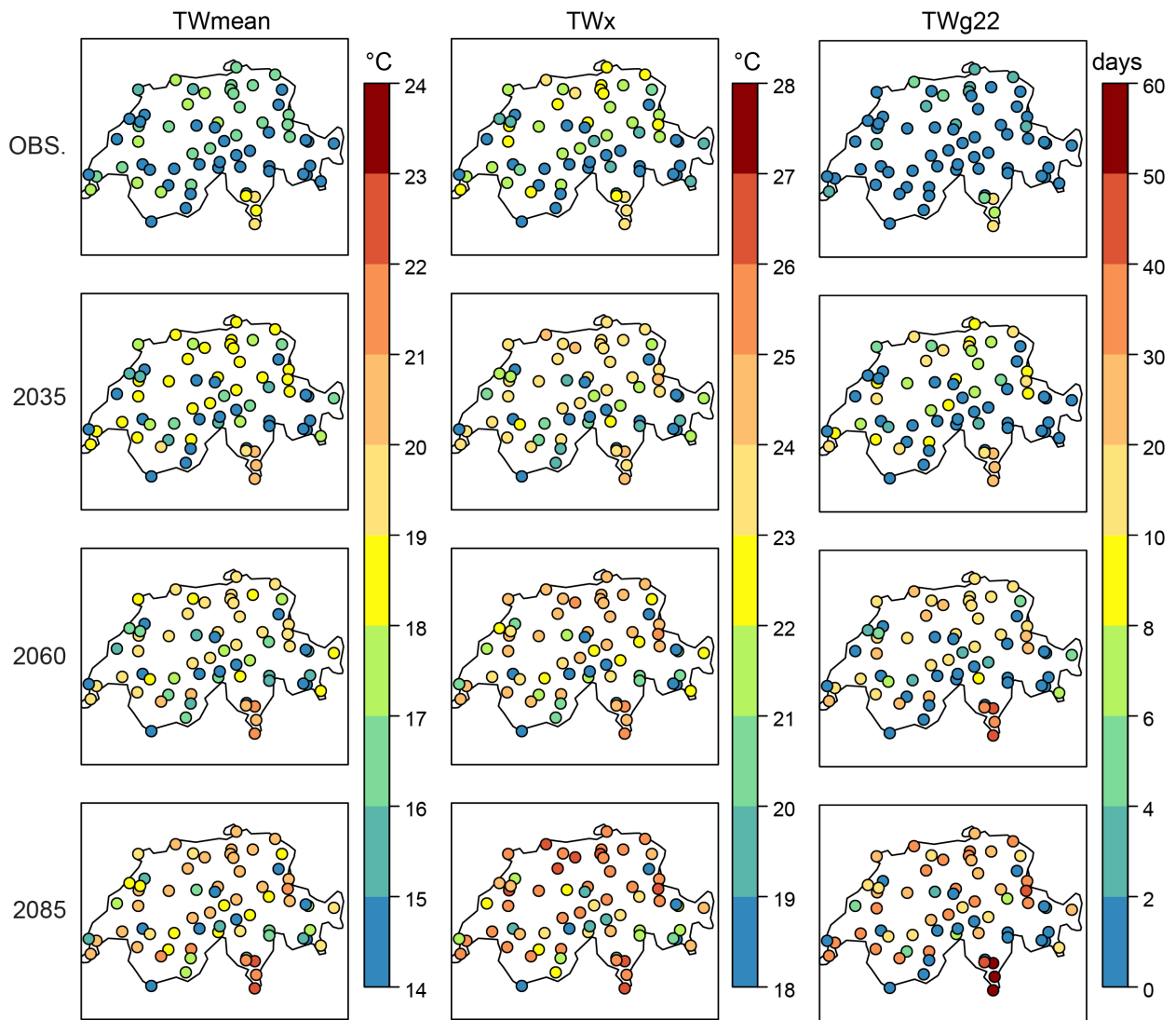
Figure 6.18. Observed values (first row) and climate-change projections (2nd - 4th rows) for summer mean (TWmean) and maximum TW (TWx) temperatures, and the number of days with TW >22 °C (TWg22) for the multi-model ensemble median for the three future periods, for the bias-corrected RCMs (combination of EUR-11 and EUR-44, 20 simulations; see Chapter 5.3) and the RCP8.5 scenario. See Figure 13.60 and Figure 13.61 for RCP2.6 and RCP4.5.

6.6. Precipitation extremes

Heavy and extreme precipitation events are of high relevance, as they may imply risk and damage to environmental and human systems. Mountainous regions like Switzerland are particularly prone to heavy precipitation and its consequences, as is evident from the August 2005 and June 2013 flood events ([228] and Chapter 3.3.3). Because the maximum amount of water vapor in the atmosphere is determined by temperature via the Clausius-Clapeyron relationship, increasing by 6 - 7 % per degree of warming, heavy precipitation events are expected to intensify at a similar rate [125, 7]. Apart from this thermodynamic effect, however, additional processes govern the future frequency and intensity of precipitation, such as changes in large-scale circulation, the occurrence of weather types, and atmospheric stratification [91, 244, 199, 260].

6.6.1. Methodology

Here, precipitation extremes are described by a set of indices that cover a broad range of characteristics. Empirical indices are used to address moderate to heavy precipitation (i.e., events that occur once to a few times per year), and indices based on extreme value statistics are used to address extreme precipitation (i.e., events that occur once per decade or century). All meteorological seasons are treated separately.

The empirical indices include the 90th, 95th, and 99th percentiles of daily precipitation ($p90$, $p95$, and $p99$) considering both wet and dry days [305]. The average maximum single-day event ($Rx1d$) and the average maximum five-day event (5-day precipitation sum, $Rx5d$) are also provided. Precipitation events that are associated with certain return periods (i.e., return levels of one-day events with a 100-year return period, $x1d100$) are estimated using extreme value statistics by fitting Generalized Extreme Value (GEV) distributions to seasonal maxima [64]. The implementation employed in CH2018 has been used in several previous studies [126, 272, 273], and similar implementations are often used in hydrology and infrastructure design. In addition to daily events ($x1dYY$), 3-day and 5-day precipitation events are considered ($x3d$, $x5d$).

6.6.2. Heavy and extreme precipitation events

Previous studies [126, 56, 272] and the most recent climate-model projections (see Figure 6.19 and [273]) agree that heavy and extreme precipitation events will intensify in all seasons and across the majority of the European continent. The most prominent and robust intensifications are found in the cold seasons and in northern Europe. Changes seen in extreme indices do not scale proportionally with changes in mean precipitation (MEA; see also Chapter 4) or the *wet-day frequency* (FRE). Changes in extreme indices are in most cases stronger than those in mean precipitation, and the wet-day frequency may even exhibit the opposite sign, especially for summer and in southern Europe. Across large parts of Europe and in most seasons, the intensification of extreme events with a return period of 100 years ($x1d100$) lies between +10 % and +30 %. Changes in moderate events ($Rx1d$) exhibit a pronounced north-south gradient pattern that is shifted with the seasonal cycle, with slight decreases in the Mediterranean region, an intensification in Scandinavia, and a transitional region with smaller changes in between. In summer, a reduction in the intensity of moderate events is seen in regions as far north as the greater Alpine region. In general, multi-day events ($Rx5d$) tend to intensify less than single-day events.
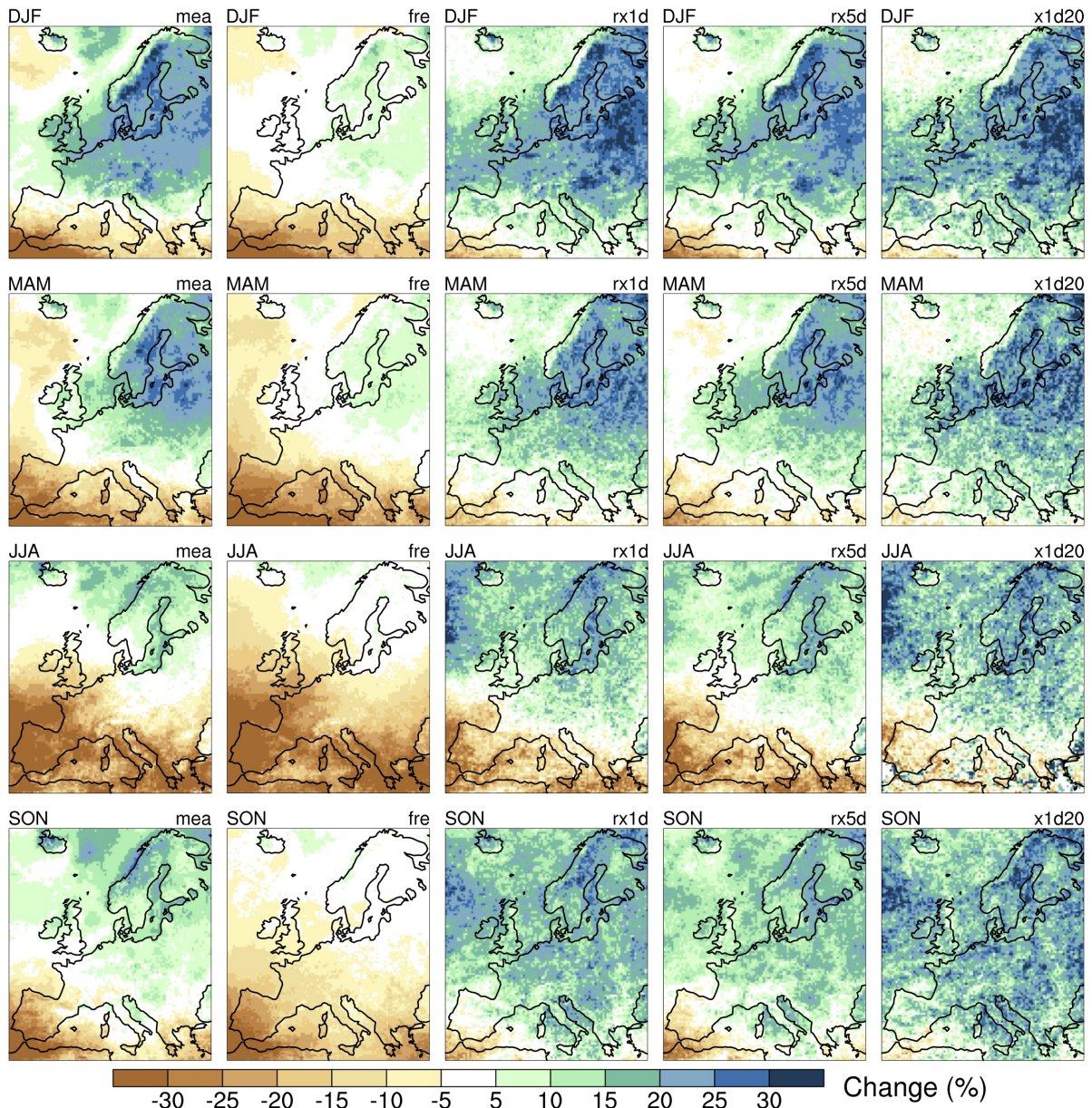
Figure 6.19. Multi-model median projected changes in (from left to right) mean daily precipitation (MEA), wet-day frequency (FRE), the mean seasonal maximum event at the daily (Rx1d) and 5-day aggregated time-scale (Rx5d), and the 20-year return value (x1d20) for each season (from top to bottom) and for RCP8.5 and the period 2085 with respect to the reference period 1981 - 2010. The multi-model ensemble consists of EUR-11 and EUR-44 simulations (see Chapter 4.2).

Heavy precipitation events are projected to intensify in all seasons and regions of Switzerland (Figure 6.20 and Figure 6.21), in particular in northern Switzerland (e.g., CHNE) and in winter (DJF). Uncertainty as indicated by the model spread is larger for extreme (e.g., *x1d100*) than for heavy or moderate events (e.g., *Rx1d*). Model spread is largest in summer (JJA) and in the south (CHS). In summer, moderate events are projected to change little, whereas extremes show a tendency to intensify, although this is not statistically significant. In other seasons, intensification across the spectra of return periods (from heavy to extreme: *Rx1d, x1d10, x1d100*) is of similar magnitude. It is further projected that in all seasons, single-day events (*Rx1d, x1dYY*) intensify more than multi-day events (*Rx5d, x5dYY*). Changes in mean seasonal precipitation (*MEA*; see also Chapter 4) scale roughly with changes in the frequency of wet days (*FRE*). However, for the most part, changes in *FRE* and *MEA* do not scale proportionally with changes in heavy and extreme events (see also [98] and Chapter 4). The degree of precipitation intensification increases with time and shows a clear trend by the end of the century. The magnitude of the projected changes depends on the emission scenario chosen (not shown) and is larger for RCP8.5 than for RCP4.5 and RCP2.6. In the near term, internal variability may dominate the response.

Overall, events that could potentially have the most devastating effects and are relevant for infrastructure planning (i.e., *x1d10* and *x1d100*) may intensify strongly in all seasons. Across Switzerland, the intensification of extreme events with a return period of 100 years (*x1d100*) lies between +10 % and +25 %, depending on the season and region (multi-model median by the end of the century in RCP8.5). However, the model spread is substantial, reflecting both internal variability and model uncertainty. At the same time, the majority of models project a reduction in the number of wet days, especially in the warm seasons (i.e., *FRE*; see also Chapter 6.7). This is of particular relevance for energy supply and agriculture. The results presented here are in line with observations from recent decades (see Chapter 3), which show a comparable scaling between mean temperature changes and heavy precipitation indices.

6.6.3. Snowfall fraction and snowfall extremes

Along with warming temperatures, the partitioning between solid (snow) and liquid (rain) precipitation will change in favor of liquid precipitation [127]. Domain and multi-model mean decreases in mean September - May Alpine snowfall by the end of the century are projected to reach about 25 % and 45 % for scenarios RCP4.5 and RCP8.5, respectively. In terms of relative changes, this effect is most pronounced in low-altitude regions (500 - 1000 m a.m.s.l), where the snowfall fraction is projected to decrease by about 70 % under RCP8.5. However, in terms of absolute changes, the effect is more pronounced in mid-altitude regions (1000 - 2000 m a.s.l.), where the corresponding decrease in snowfall is projected at about 0.6 - 1.0 mm/d (RCP8.5 multi-model mean). There are considerable uncertainties in this estimate stemming from the separation of precipitation into snowfall and rainfall.

The decrease in the snowfall fraction will also decrease the probability of large snowfall events in low- to mid-altitude ranges. In contrast, high-elevation regions (> 2000 m a.s.l.) could experience slight snowfall increases in mid-winter for both the RCP8.5 and RCP4.5 emission scenarios, despite the general decrease in the snowfall fraction [127]. These increases in mean and heavy snowfall can be explained by a general increase in winter precipitation.

The projected reduction of the snowfall fraction in low and intermediate altitude ranges is of concern, as it implies – together with the earlier melt of the snowpack – changes in runoff behavior, with increasing mean runoff in winter and early spring and decreasing runoff in late spring and summer [115, 33]. There is evidence that these changes will raise the risk of both floods and low flows, but the behavior will strongly depend upon the catchment considered; this aspect will further be addressed in Hydro-CH2018 (see Chapter 10).
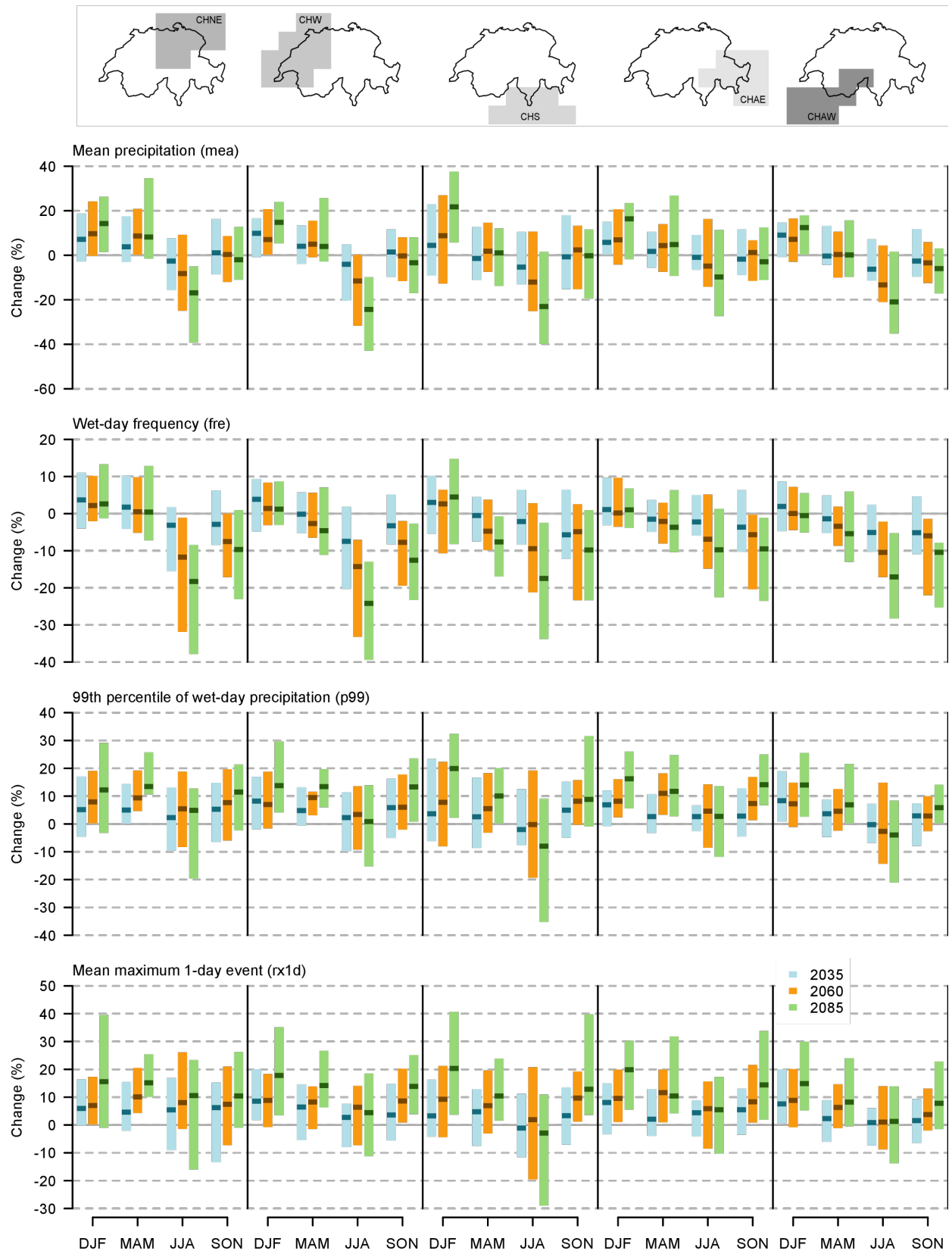
Figure 6.20. Multi-model ensemble projected changes in mean daily precipitation (MEA), wet-day frequency (FRE), the 99th percentile of all-day precipitation (p99), and the mean seasonal maximum daily precipitation event (Rx1d) for all seasons (see x-axis) for the five CH2018 analysis regions, for RCP8.5 and the periods 2035 (blue), 2060 (red), and 2085 (green) with respect to the reference period 1981 - 2010. The multi-model ensemble consists of EUR-11 and EUR-44 simulations (see Chapter 4.2).
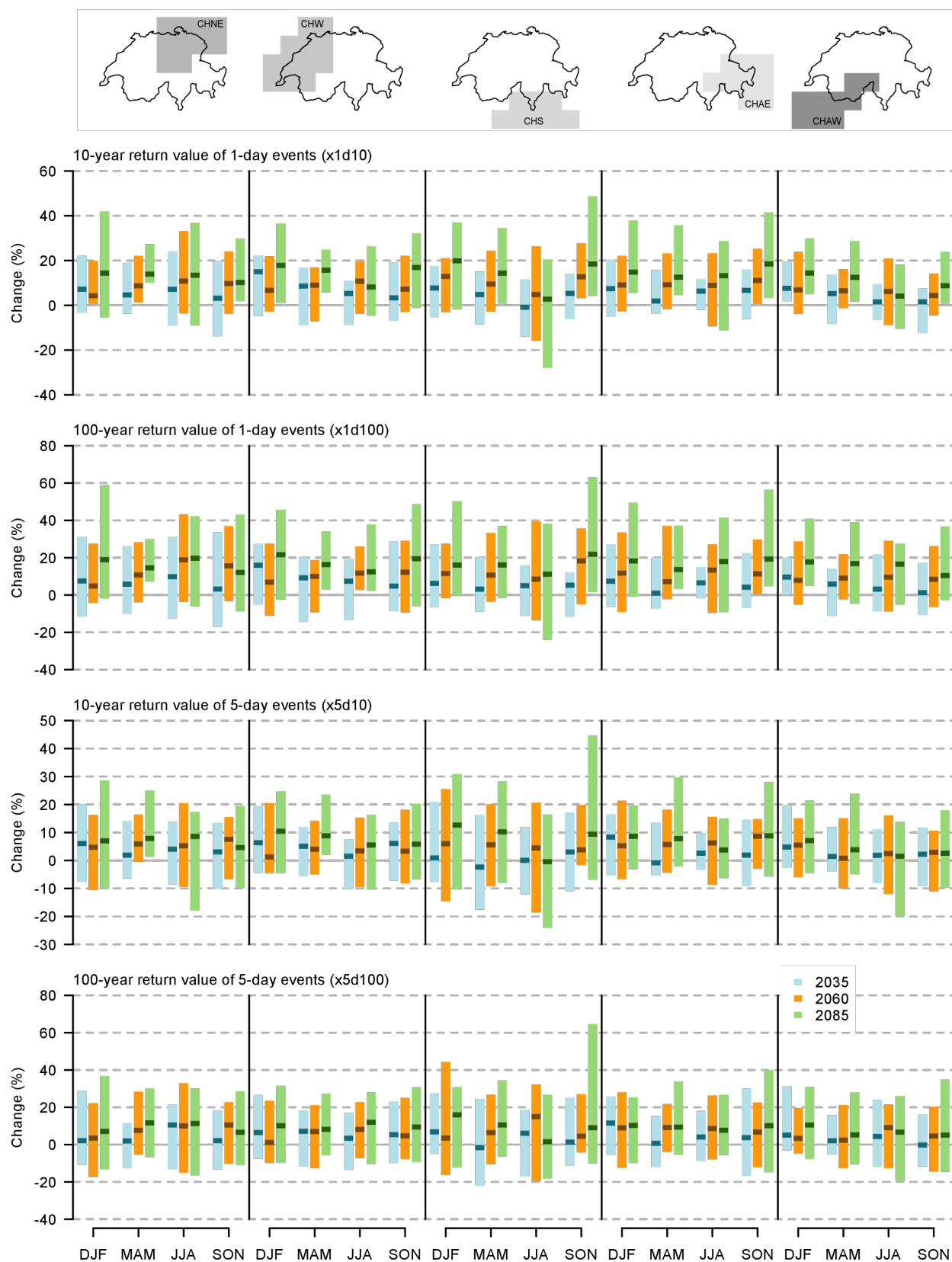
Figure 6.21. Multi-model ensemble projected changes in the intensity of daily events with a return period of 10 years (x1d.10) and 100 years (x1d.100) and the corresponding events for 5-day aggregated precipitation episodes (x5d.10 and x5d.100) at seasonal scale (see x-axis) for the five CH2018 analysis regions, for RCP8.5 and the periods 2035 (blue), 2060 (red), and 2085 (green) with respect to the reference period 1981 - 2010. The multi-model ensemble consists of EUR-11 and EUR-44 simulations (see Chapter 4.2).

Box 6.1: Hourly precipitation extremes & convection-resolving climate simulations

The CH2018 climate-change projections largely rely on Regional Climate Models (RCMs). Due to the models' coarse horizontal resolution (12 km - 50 km), they suffer from limitations associated with small-scale unresolved processes (thunderstorms and rain showers, i.e., convective precipitation) and have difficulties representing the complex topography of Switzerland. Increasing the horizontal resolution of RCMs to the kilometer scale (< 4 km) allows switching off the parameterization of convection, which is one of the key sources of uncertainty in future projections of extreme precipitation. These Convection-Resolving Models (CRMs) are currently in use for Numerical Weather Prediction (NWP), but with recent model developments and advances in computational power, it has become feasible to use such resolutions for climate studies as well.

Some of the first decade-long convection-resolving simulations have been conducted over the southern part of the United Kingdom [183] and over the greater Alpine region [12]. Evaluation of these simulations has revealed that convection-resolving models significantly improve the simulation of precipitation, especially for heavy precipitation on hourly timescales [12, 183]. As an example, Figure 6.22 shows the diurnal cycle of mean precipitation, wet-hour frequency, and heavy precipitation (defined as the 99th percentile of all hours), averaged over 62 surface precipitation stations across Switzerland and simulated by a convection-resolving model at a horizontal resolution of 2.2 km over the greater Alpine region. The convection-resolving model is compared to rain-gauge station observations and a convection-parameterizing model at a horizontal resolution of 12 km. The results from convection-resolving models show great improvements in the timing of precipitation, precipitation frequency, and the simulation of peak heavy precipitation. Convection-parameterizing models tend to produce too frequent precipitation with small intensity, and excessively early precipitation peaks. They are thus inadequate for assessing potential changes in hourly precipitation intensity under conditions of climate change.
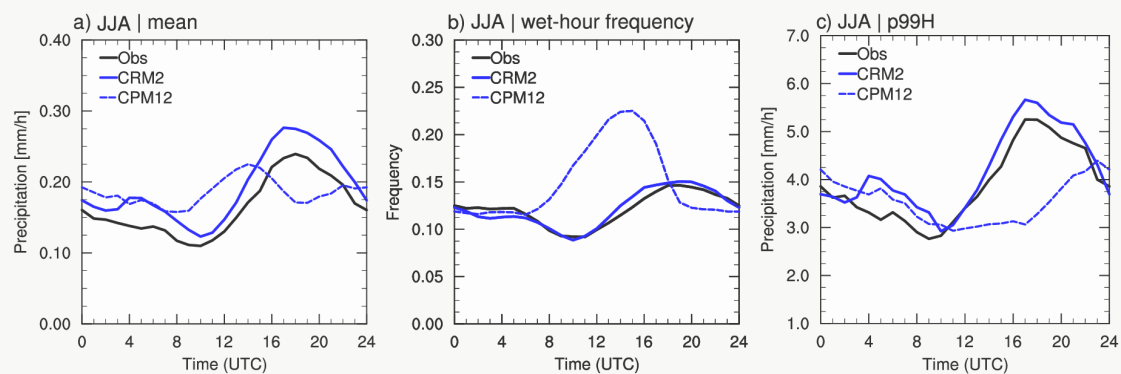

Figure 6.22. Diurnal cycle of (a) mean precipitation, (b) precipitation frequency, and (c) heavy precipitation (defined as the 99th percentile of all hours) obtained in the convection-resolving simulation at 2.2-km horizontal resolution (CRM2), convection-parameterizing simulation at 12-km horizontal resolution (CPM12), and observations from rain-gauge stations. The evaluation is performed for the summer (JJA: June - July - August) season, and the results are averaged over 62 stations across Switzerland. Results are based on 10-year-long high-resolution simulations presented in [12, 13].

Convection-resolving and convection-parameterizing climate-change simulations (driven by one specific RCP8.5 GCM) of summer precipitation over the greater Alpine region are shown in Figure 6.23. Following Ban et al. (2015) [13], relative changes in extreme summer precipitation are expressed in relation to mean temperature change, i.e., as a scaling rate. A comparison of the convection-resolving and convection-parameterizing models shows small differences in changes in extreme precipitation at daily scales, but large differences at hourly timescales. The increase in extreme hourly precipitation is smaller in the convection-resolving model than in the convection-parameterizing model.

Furthermore, the convection-resolving model shows that increases in extreme hourly precipitation, similar to extreme daily precipitation, is actually consistent with the Clausius-Clapeyron rate, i.e., the increase in the most extreme events converges toward a value of about 6.5 % K^{-1} (Figure 6.23) [13]. The convection-parameterizing model suggests that the increase in extreme hourly precipitation may exceed the Clausius-Clapeyron rate; however, this result is not reliable, since the model has difficulties reproducing extreme hourly precipitation [12, 13]. The increase in extreme hourly precipitation in convection-resolving models is also smaller than what might be expected from the present-day scaling found in observations, which exceeds the Clausius-Clapeyron rate (i.e., 6 - 7 %K^{-1}) in the summer season [12]. Thus, the results indicate that convection-resolving model projections are

consistent with theoretical expectations from the Clausius-Clapeyron relationship; moreover, future changes in extreme hourly precipitation cannot be extrapolated from present-day precipitation scaling, but they are likely to follow the Clausius-Clapeyron scaling of 6 - 7 %K^{-1}. This comparatively simple scaling law can be used for a number of climate-change adaptation strategies [13].
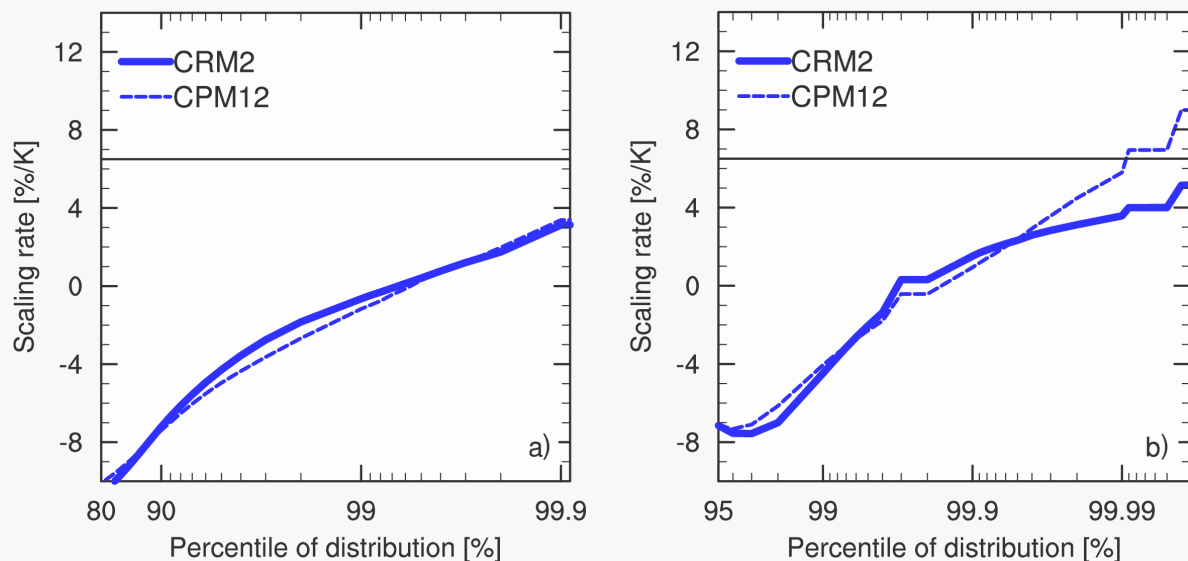

Figure 6.23. Projected changes in precipitation intensity as a function of percentiles, normalized by the local temperature changes for convection-resolving (CRM2, resolution of 2.2 km, solid lines) and convection-parametrizing (CPM12, resolution of 12 km, dashed lines) models [13], calculated for (a) daily precipitation and (b) hourly precipitation, averaged over the greater Alpine region. (From [13]).

The future warming of the atmosphere will also lead to changes in other hazardous convective events, such as tornadoes, hailstorms, and severe thunderstorm winds. Some studies have explored the use of convection-resolving models for the simulation of such events in a future climate, but the results are still very limited. However, they indicate that future increases in summer precipitation over high alpine elevations are associated with enhanced convection, as found in both conventional and convection-resolving climate simulations [132]. Studies over Colorado's mountains indicate that despite more intense convection in a warmer climate and more hail generated within clouds, less hail reaches the surface due to the enhanced melting associated with climate warming [209]. More robust results are found using global and regional climate models, which show that the further warming of the atmosphere will lead to increases in the occurrence of severe thunderstorms [81] and can also result in increases in the frequency of lightning strikes [281].

6.7. Drought indices

Measuring and defining drought is not straightforward, as the term can be defined in various ways, depending on the perspective of the stakeholders. Commonly, one distinguishes between meteorological drought, which refers to a deficit of precipitation, soil moisture drought (often called agricultural drought), which refers to a deficit of (mostly root zone) soil moisture, and hydrological drought, which refers to negative anomalies in streamflow, lake, and/or groundwater levels (e.g., [152]). These multifaceted definitions of drought and the lack of direct measurements of drought-related variables, in particular soil moisture (e.g., [315, 84]), have led to the development of several indices to characterize (meteorological, agricultural, and hydrological) drought (see, e.g., [152, 70]). It should be noted that such indices are not necessarily restricted to depicting dryness, but can also represent wet conditions.

Lack of precipitation is often the primary cause of drought; this is the basis for the definition of meteorological drought indices that reflect the aspect of a water deficit on the supply side (see Figure 6.24). On the demand side, increased evapotranspiration induced by enhanced radiation, wind speed, or a vapor pressure deficit (itself linked to temperature and relative humidity) can further intensify the water shortage and lead to critical soil moisture values and the associated agricultural drought. Under strong drought conditions, however, soil moisture can also become limiting for evapotranspiration, which can restrict

further soil moisture depletion. Furthermore, pre-conditioning (pre-event soil moisture, surface and/or groundwater storage) can contribute to the emergence of agricultural and hydrological droughts. This is related to the inherent characteristic memory of these water stores (e.g., [196, 310, 250]) and their specific response times to drought forcing (e.g., [113]).
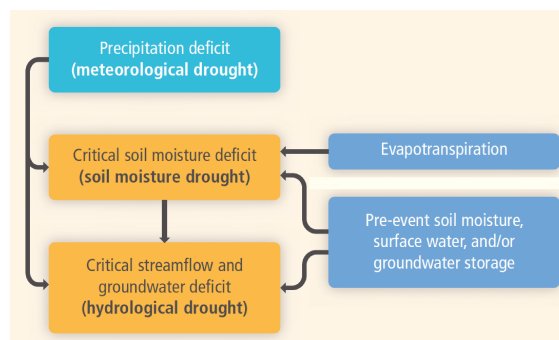

Figure 6.24. Schematic of the different climatic drivers of meteorological, agricultural (soil moisture), and hydrological drought (from [311]). Light blue relates to supply-driven impacts on the different types of drought, dark blue to demand- or storage-driven impacts.

Switzerland has experienced several drought episodes since the beginning of the 20th century. Long-term historical trends are insignificant, although they indicate a tendency toward drying (i.e., negative trend slope of standardized precipitation minus evapotranspiration; see Chapter 3.3.3). Climate change will affect the drivers of drought via the modification of atmospheric circulation and associated precipitation patterns, as well as via changes in radiation, air temperature, atmospheric humidity, and wind (e.g., [314]; see Figure 2 therein). Thus, to investigate the different impacts of climate change on drought, it is appropriate to use indices covering multiple drought definitions (see also [311]). Here, the focus is on meteorological and agricultural drought, as these can be more directly derived from the CH2018 climate model projections than hydrological drought. Two meteorological and two agricultural drought indices are considered (see Table 6.1).

6.7.1. Meteorological drought (precipitation deficits)

The *consecutive dry days* index (*CDD*) shows the maximum number of consecutive days without rain (i.e., below a given threshold, typically 1 mm d^{-1}) within a considered period [128, 6, 337]. Here, *CDD* is calculated on a seasonal timescale (i.e., for DJF, MAM, JJA, or SON as a whole). Another commonly used meteorological drought index is the *standardized precipitation index* (SPI; [222, 205]). This is derived by fitting and transforming a long-term precipitation record into a normal distribution that has zero mean and unit standard deviation. SPI values of -0.5 to -1 correspond to mild droughts, -1 to -1.5 to moderate droughts, -1.5 to -2 to severe droughts, and below -2 to extreme droughts. Similarly, values from 0 to 2 correspond to mildly wet to severely wet conditions, and values above 2 to extremely wet conditions. SPI can be computed over several timescales (e.g., 3, 6, 12, or more months) and thus indirectly considers effects of accumulating precipitation deficits. Here, the 3-month timescale is used (3-month SPI, denoted *SPI3*). The index is calculated separately for each month and then seasonally averaged. SPI only considers the supply of moisture, which is currently sufficient for western to central Europe. However, in southern Europe, the effects of evapotranspiration need to be considered as well for an appropriate representation of water deficit [269].

6.7.2. Agricultural drought (soil moisture deficits)

Precipitation minus evapotranspiration (*P-E*) describes the net flux of water between atmosphere and land by including the influence of both atmospheric supply and demand (Figure 6.24). Here, seasonal averages of *P-E* are considered to represent water availability [136, 47]. Actual evapotranspiration, which results from atmospheric forcing and simulated soil moisture limitation on evapotranspiration, is used; compared to potential evapotranspiration, it is less prone to overprediction [233]. The index is categorized as an agricultural drought index, although it neglects storage changes and runoff. The fact that most of the

CORDEX simulations employ aerosol climatologies that remain constant at late 20th-century levels (see also [Chapter 4.2](#)) probably leads to an underestimation of the radiation forcing in the regional projections (see [15]) and the consequent impacts on evapotranspiration. *Standardized soil moisture anomaly* (*SMA*) is an alternative measure for the evaluation of agricultural drought based on simulated total column soil moisture (e.g., [71, 249]). Monthly *SMA* values are calculated with respect to the monthly means of the reference period and standardized by the monthly standard deviations of the reference period [248]; these values are then seasonally averaged. *SMA* integrates the effects of precipitation forcing, simulated evapotranspiration (see above), and simulated soil moisture persistence. Although the soil moisture simulated by (land-surface, hydrological, and climate) models often exhibits strong discrepancies in absolute terms, soil moisture anomalies can be compared by simple scaling and generally match reasonably well (e.g., [195, 248]). Recent studies furthermore suggest that future drought projections should rely on direct climate-model output of the water cycle (e.g., simulated soil moisture, as used for *SMA*), as a posteriori off-line metrics tend to overestimate drying trends (e.g., [26, 234]).

[Figure 6.25](#) shows the ensemble median changes in the meteorological and agricultural drought indices on
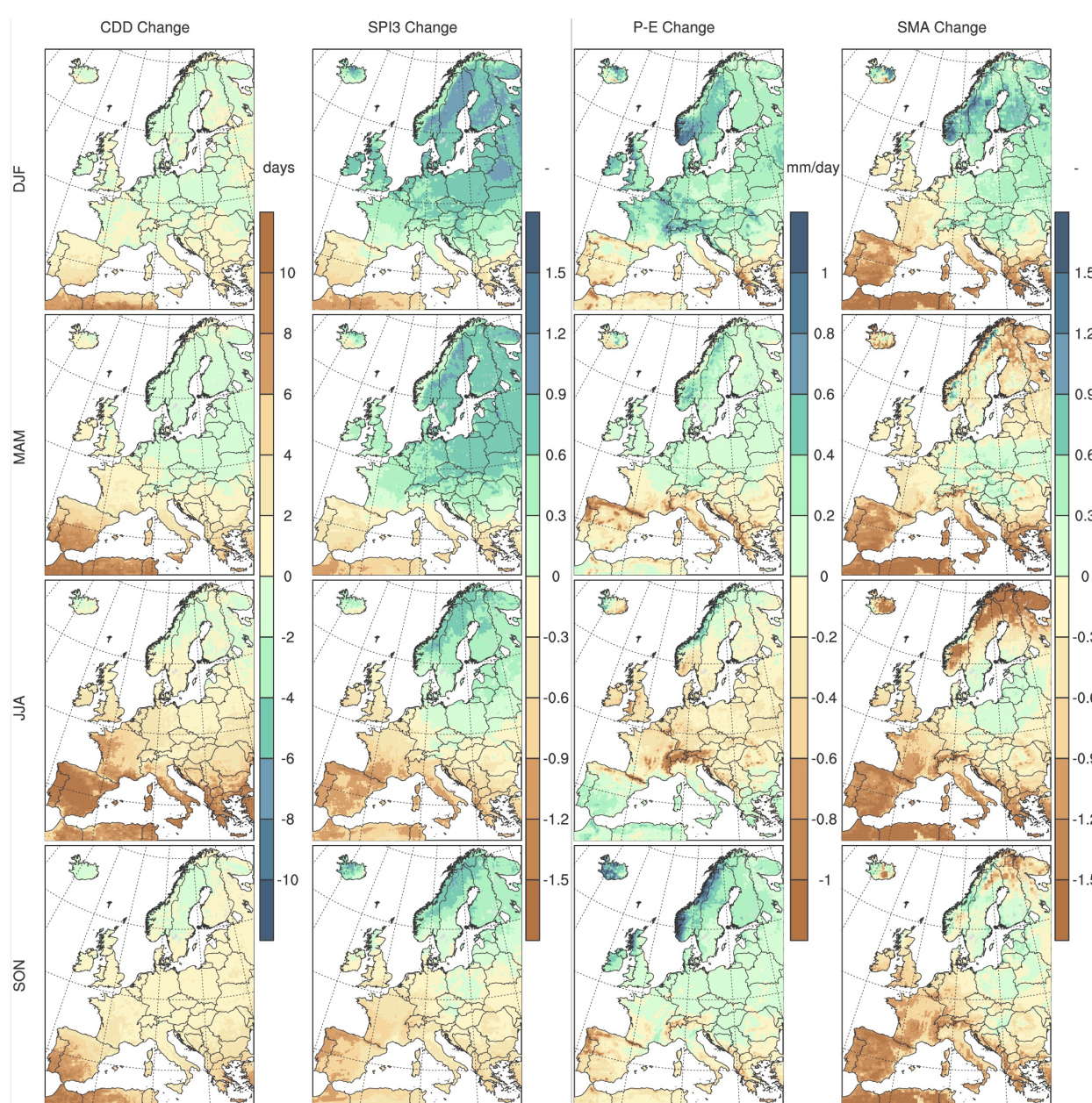

Figure 6.25. Ensemble median changes in the meteorological and agricultural drought indices CDD, SPI3, P-E, and SMA (from left to right) for the different seasons (top to bottom) and the RCP8.5 emission scenario by 2085. The ensemble median is based on a combination of EUR-11 and EUR-44 simulations ([Chapter 4.2](#)).

the European scale under the RCP8.5 emission scenario by 2085. *CDD* indicates increasing dry spell lengths in the Mediterranean and western/central Europe. The signal shows a northward shift over the course of the year (i.e., extending further north in summer) and toward the later scenario periods (not shown). Similarly, *SPI3* also displays an intensification and extension of a drying trend in the Mediterranean and western Europe, with stronger and extended signals in summer and again for the later scenario periods (not shown). In northern Europe, *SPI3* shows a wetting trend that is more extended in winter/spring and intensifies in the 2085 scenario period. The European-scale analysis indicates that Switzerland is often in between the drying (in summer/autumn) and wetting signals (in winter/spring). This position within the larger-scale change signals points to the inherent uncertainties associated with regional responses within the CH2018 regions (see below).

The agricultural drought indices *P-E* and *SMA* both show a drying in the Mediterranean and western Europe, again intensified for the 2085 scenario period (not shown) and more extended in summer. Similar to *SPI3*, the agricultural drought indices also indicate a wetting trend in parts of northern Europe, in particular for winter and in the 2085 scenario period. In summer, *P-E* shows effects of water limitation in the southern Mediterranean (e.g., over the Iberian Peninsula), where the net change in the index becomes positive due to a strong decrease in evapotranspiration. Overall, the agricultural drought indices suggest more heterogeneous signals than the solely precipitation-driven meteorological drought indices. For *SMA* (and, to a lesser extent, for *P-E*), topographical effects can be observed as well. Mountainous regions (e.g., in the Alps and in Scandinavia) seem more prone to drying, which appears to be related to carry-over effects due to less snow storage and earlier spring snow melt, in connection with increased runoff (not shown). In parts of Scandinavia, this runoff effect even seems to result in a net soil drying despite increased *P-E*.
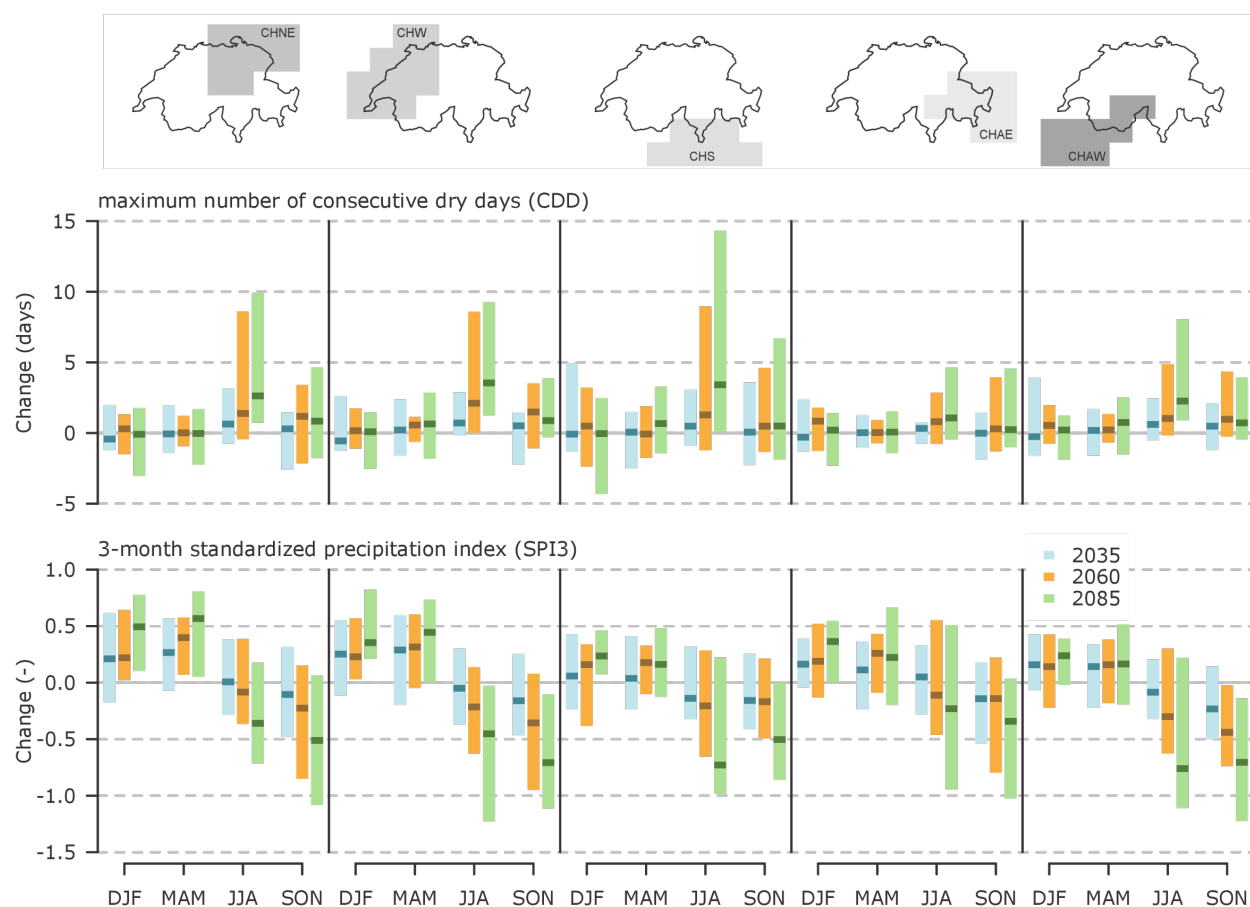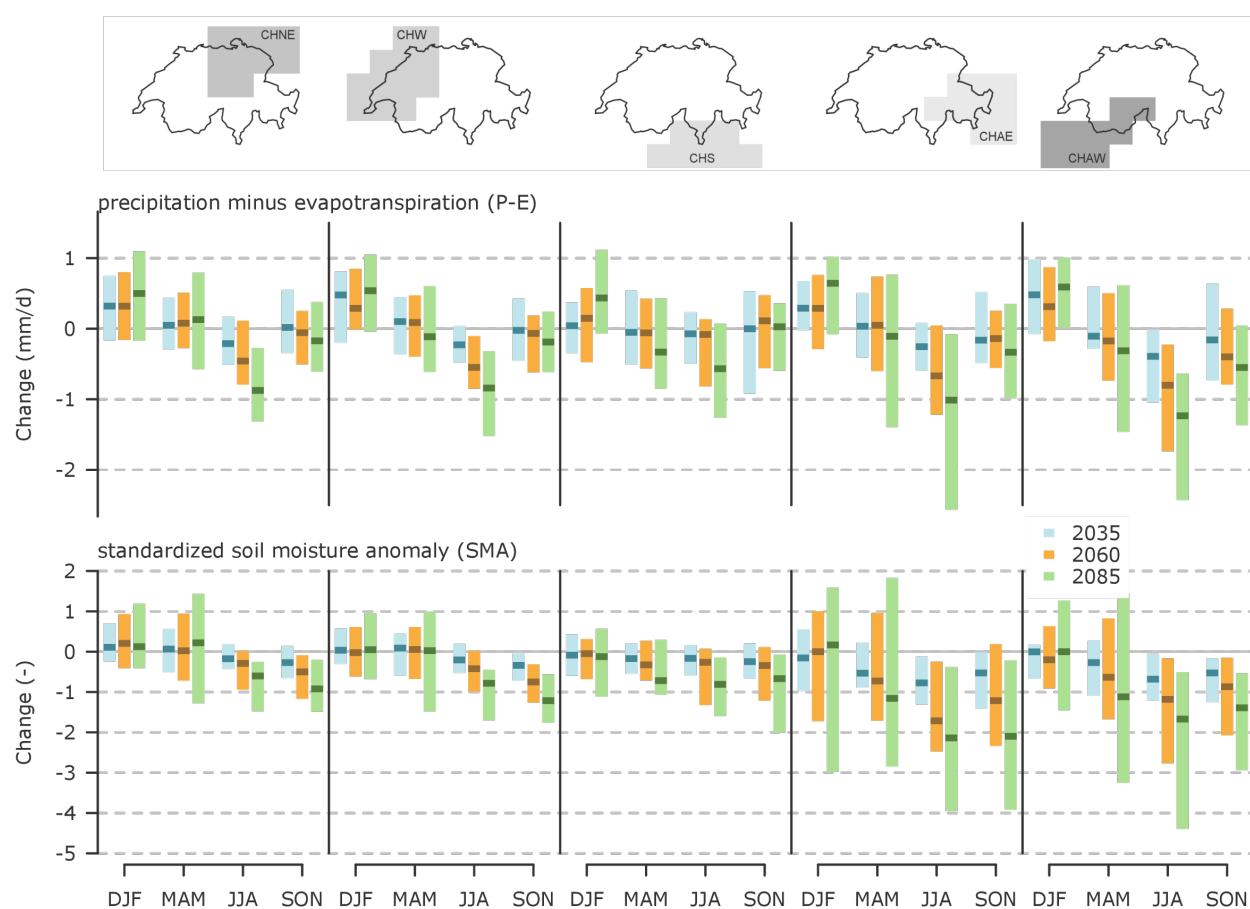

Figure 6.26. Multi-model regional mean changes in the meteorological drought indices CDD (top) and SPI3 (bottom) for the five CH2018 regions and the scenario periods 2035, 2060, and 2085 and RCP8.5. The ensemble median is based on a combination of EUR-11 and EUR-44 simulations (Chapter 4.2). See Figure 13.66 and Figure 13.67 for RCP4.5 and RCP2.6.

For most CH2018 regions (except CHAE) and primarily for the period 2085, *CDD* exhibits a signal toward longer dry spell lengths in summer for RCP8.5 (possible increases of up to 8 - 14 days from the currently observed 11 days on average; Figure 6.26, top). These signals are, however, associated with larger uncertainties, and neither weak nor strong changes can be excluded. The other seasons do not show significant changes in this index. *SPI3* shows a winter/spring wetting that often intensifies by the end of the century (Figure 6.26, bottom). This signal manifests in all CH2018 regions and becomes pronounced for CHNE and CHW in particular; it is less evident in CHS and in the Alpine regions CHAE and CHAW. For summer and autumn, the signal for *SPI3* is less consistent. The median estimate indicates a drying in the later periods for all regions and both seasons. The models project a consistent drying in CHW (summer and autumn) and in CHAW (autumn) for the period 2085, but the signal is associated with uncertainties in the sign of the change in the other regions (i.e., a minority of models also project a wetting). Overall, uncertainty ranges in summer are larger than in other regions, due to the fact that Switzerland is situated in between the larger-scale change wetting and drying signals (see Figure 6.25), with individual models projecting diverse or even opposite responses.

Figure 6.27. Multi-model regional mean changes in the agricultural drought indices P-E (top) and SMA (bottom) for the five CH2018 regions and the scenario periods 2035, 2060, and 2085 and RCP8.5. The ensemble median is based on a combination of EUR-11 and EUR-44 simulations (Chapter 4.2). See Figure 13.66 and Figure 13.67 for RCP4.5 and RCP2.6.

In agreement with *SPI3*, the agricultural drought index *P-E* shows a tendency toward a wetting in winter by the end of the century in all CH2018 regions under RCP8.5 (Figure 6.27, top); however, this signal is not as pronounced, and some models also project insignificant changes. For summer, *P-E* shows a drying, which becomes most evident for the 2085 scenario period (except in CHS, which shows uncertainty in the sign of the change). This summer drying also appears in *SMA* (Figure 6.27, bottom), which exhibits a decrease by the end of the century in all CH2018 regions. In addition, *SMA* also shows a drying in autumn. Overall, the two agricultural drought indices exhibit larger uncertainties in the two Alpine regions, likely associated with the complexity of the underlying snow and precipitation, evapotranspiration, and storage processes that govern the responses of these indices.

Considering RCP2.6 (see [Appendix 3.5](#)), the changes for *CDD* and *SPI3* are not robust, with various models projecting opposite signs of change. For RCP4.5, *CDD* exhibits a tendency toward longer dry spell lengths in summer, in particular for the western part of Switzerland (CHW and CHAW). The changes are, however, less strong than for RCP8.5. For *SPI3*, a tendency for spring wetting can be observed in CHNE only in the later two scenario periods under RCP4.5. *P-E* also shows mostly non-robust responses for the lowest emission scenario, while for RCP4.5, an indication of summer drying appears in CHNE, CHW, and CHAW. *SMA* starts to show a tendency toward summer drying for RCP2.6 in CHAE in the 2085 period. This signal intensifies under RCP4.5 and also expands to CHAW under this scenario.

In summary, for Switzerland under RCP8.5, the drought indices considered here show a tendency toward an increase in dry spell lengths (*CDD*) and tendencies toward drying in summer (*SPI3*, *P-E*, *SMA*), as well as wetting in winter (but only when storage effects are neglected, i.e., for *SPI3* and *P-E*). The extent of the drying seems to be partially dependent on the index and on the domain, and the signal is most visible by the end of the century. The clearest responses are observed when effects of atmospheric demand and storage are included in the index (as is the case for *P-E* and *SMA*). Overall, the level of drying remains uncertain, and both insignificant and very strong changes cannot be excluded. This is related to large internal variability and model uncertainties in the representation of key processes (e.g., strength of soil moisture-atmosphere feedbacks, circulation changes), as well as factors such as aerosol forcing, irrigation, and land-use changes that may differ between models and multi-model experiments (see also [Table 6.2](#)). It should be noted that the CH2018 domain is often in between the European-scale signals (i.e., winter wetting in northern Europe, summer drying in southern Europe), and thus the responses in the individual Swiss regions depend on their location with respect to the larger-scale signal.

6.8. Wind extremes

A good knowledge of the frequency and geographical distribution of extreme winds is key for the prevention of damage caused by windstorms. Unfortunately, for the highly complex topography of Switzerland, our current knowledge on extreme winds and their evolution over time is still rather limited. As shown in [Chapter 3.2.4](#), near-record wind gusts in Switzerland can be caused by winter storms, summer convection, and flow crossing the main Alpine ridge (Föhn) or deflected flow such as the Bise (cf. [Figure 3.11](#)).

To give a preliminary overview of the current state of knowledge regarding wind extremes (especially winter storms), we summarize the findings of earlier studies focusing on Europe and Switzerland. Several review studies have indicated that in the second half of the 21st century, the frequency and intensity of storms, cyclones, and high-impact wind might increase over central and western Europe, resulting in a high potential for associated damages [389, 355, 96, 241]. This is in contrast to southern Europe, where current model projections indicate a future decrease in extratropical storminess [241]. This picture becomes more complicated when one considers only the seven CMIP5 simulations that show the best performance in simulating historical mean wind fields over Europe. In this regard, Colle et al. (2013) [65] found a decrease in cyclone track density and a weakening of cyclones over the western Atlantic storm track. This has been confirmed in a recent study by Wang et al. (2017) [365], although their work is based on a large ensemble with only one climate model. The reason for this diversity of results lies in the nature of the phenomenon being analyzed, as different processes (such as a projected decrease in meridional temperature gradient in the lower troposphere or an increase in humidity) can have opposing impacts on storm track responses. This makes future projections of extratropical cyclones and thus wind extremes a challenge [319].

Another important process leading to high-impact wind extremes is the serial clustering of extratropical storms over the North Atlantic European area [210, 30, 29]. Economou et al. (2015) [88] showed that future changes in serial clustering are generally found to be small and are not consistent across CMIP5 models. Multi-model ensembles of RCMs generated in earlier projects such as PRUDENCE and ENSEMBLES agree with the diverse picture highlighted by the GCM simulations. Still, model studies show that there is some

indication of an intensification of wind extremes over western or central Europe that could also affect northern Switzerland (cf. [25, 278, 303, 83, 134, 252]). The analysis of wind extremes in this report is based on the CORDEX multi-model ensemble, as described in Box 2.1. Like the earlier multi-model ensembles of RCMs, the CORDEX RCMs are able to simulate the large-scale wind patterns above the boundary layer, but are not yet capable of resolving all relevant phenomena causing extreme near-surface (10-m) winds. An evaluation of the 10-m mean wind speed at MeteoSwiss observational sites reveals substantial biases on the annual and seasonal scales during the reference period (1981 - 2010). For example, some of the ensemble members are unable to simulate the spatial structure and the seasonal cycle of the 10-m mean wind field in the complex Alpine topography. Thus, the surface wind data of the CORDEX multi-model ensemble must be treated and interpreted with caution, and we recommend use of this data only after consultation with the authors of the CH2018 report.

To gauge whether there are any signs of trends in the CORDEX wind data over Switzerland, changes in the 98th percentile of daily maximum wind speeds have been computed for the CORDEX multi-model ensemble. The results for the EUR-11 model ensemble show only very small changes over Switzerland in all scenarios and for all time periods. The relative changes in the mean 98th percentile over all grid points in Switzerland in the RCP8.5 scenario range between -1.9 % and +1.8 % depending on the model for the period around 2035, between -1.6 % and 1.8 % around 2060, and between -2.5 % and +1.8 % around 2085. For the other scenarios, the changes are even smaller.

In summary, we conclude that given the complexity of the processes involved in generating wind extremes [319] and the fact that Switzerland is located in an area between projected increases (over central Europe) and decreases (over southern Europe) in storminess, it currently remains unclear whether and how wind extremes over Switzerland will change in response to anthropogenic climate forcing.

6.9. Conclusions and implications

This chapter provides a comprehensive and quantitative assessment of changes in weather and climate extremes in Switzerland. While extreme events are a natural element of the climate system, their frequency, intensity, and character will change in response to climate change. Here, we provide different lines of evidence from observations, models, and theory that demonstrate that many weather and climate extremes are changing significantly with increasing atmospheric greenhouse-gas concentrations and global warming (Table 6.2). Switzerland is expected to experience the following changes in extreme events:

- As average temperatures continue to increase, there will very likely be more frequent, more intense, and longer-lasting heat waves and extremely hot days, weeks, and seasons in all the RCPs considered. Along with central and southern Europe, Switzerland is a hotspot for changes in hot temperature extremes, as it has experienced one of the strongest intensifications of hot extremes worldwide over recent decades and is projected to experience some of the strongest intensifications of hot extremes also with future warming. The magnitude of the changes strongly depends on the RCP and is much larger for RCP8.5 than for RCP4.5 and RCP2.6.

- There will very likely be more frequent days with high heat stress due the combined effects of temperature and humidity, and similar increases are projected for very warm nights. These changes are largest at low elevations where the population density is typically highest, and the heat stress may be further amplified by urban heat island effects. Particularly in RCP4.5 and RCP8.5, heat stress is projected to reach levels that have not been observed over the past century, implying potentially adverse impacts on public health, labor productivity, and livestock. *There will likely be more frequent and intense heavy rainfall events with warming temperatures. Heavy rainfall events are projected to become more frequent and intense in all seasons, but particularly in the winter half year, at a rate that is substantially higher in RCP8.5 than in RCP4.5 and RCP2.6. Heavy rainfall events, from hourly downpours to multi-day periods, continue to increase with warming temperatures, a projected trend for which now also observational evidence exists for daily extremes. The most intense of the events experience the strongest

intensification. At the station or grid-point level, these changes are superimposed by high internal variability and are thus only significant for long periods or high warming levels. The intensification broadly follows the capacity of warmer air to carry about 6 - 7 % more moisture per degree of warming. Confidence in heavy rainfall intensification is now higher, given the evidence from observations and from a new generation of climate models run at unprecedented resolution. Along with a higher snow line, associated with a shift from solid (snow) to liquid (rain) precipitation at higher elevations, the intensification of heavy rainfall has implications for the risk of flooding.

- There is a tendency toward longer dry spells (periods with no rain) in summer (a majority of models in RCP4.5 and RCP8.5) and toward more pronounced agricultural droughts in summer and autumn by the end of the 21st century (likely – most of the models in RCP8.5). The extent of the drying remains uncertain (both insignificant and very strong changes cannot be excluded) and depends in part on the region. Switzerland is located between southern Europe that is projected to experience a severe increase in drought risk, and northern Europe that will receive more winter precipitation.

- There will very likely be fewer and less intense cold waves, *frost days*, and *ice days* with warming mean winter temperatures, particularly in RCP4.5 and RCP8.5. These changes are largest at higher elevations and are potentially amplified by snow-albedo feedbacks. Impacts may be both positive (for instance, due to reduced energy demand for heating or alleviated adverse health effects) and negative (due to an increase in pests). Given the very high natural internal variability of winter temperatures, cold winter periods will continue to occur for several more decades.

By the second half of the 21st century, changes in extremes are highly dependent on the level of warming and thus on the emission scenario. The number of extreme events depends non-linearly on the level of warming, such that any additional degree of warming will have a substantially stronger effect. It should be noted that at the scale of Switzerland, long-term trends in the frequency, intensity, and duration of extreme events are associated with large decadal and multi-decadal variability, which can lead to the absence of certain events for several decades and likewise to a clustering of several severe events in other decades. However, particularly in the long term, the trends in weather and climate extremes are expected to emerge clearly in Switzerland and also consistently affect the neighboring countries. In the near term, the intensity and frequency of extreme heat anomalies will very likely change within decades, whereas changes in the extremes of the water cycle (beyond changes in the snow line) might be dominated by natural fluctuations for several decades.

Type of extreme	Process-based expectation	Observed changes over last decades	Projected changes	LOSU*	Key uncertainties in projections
Hot days and warm nights in summer	More frequent and warmer hot days and warm nights as a result of mean summer warming, strongest increase at low elevations and areas of low variability	More hot days, summer days, warm nights and tropical nights (Section 3.4.2)	More summer days and tropical nights, strong increase in very warm days and nights (Section 4.3.3 and 4.3.4)	Very high	Amplification due to urban heat island effects, soil moisture-temperature feedbacks, circulation changes, and lack of consideration of changes in land use and irrigation.
Heat extremes, summer heatwaves	Increasing intensity of heat extremes and more frequent and longer lasting heatwaves along with summer warming and enhanced variability/amplification through land-atmosphere interactions	Increasing intensity of heat extremes and increasing frequency and duration of heat waves (Section 3.4.2)	Increasing frequency, intensity and duration (Section 4.3.3 and 4.3.4)	High	Circulation changes (persistence of anticyclones, large-scale circulation changes), strength of land-surface atmosphere interactions, precipitation and cloud processes
Heat stress (combination of temperature and humidity)	More frequent and intense heat stress due to higher temperatures and specific humidity which increases despite a weak reduction in relative humidity	?	More intense and more frequent days with high heat stress (Section 4.3.5)	High	Same as for heat extremes, other factors affecting heat stress such as changes in wind, radiation and urban heat island effect
Cold days and nights in winter	Fewer and warmer cold days and nights as a result of mean winter warming, strongest reduction at high elevations and areas of snow melt or shortening snow seasons	Fewer and warmer cold days and nights in winter, fewer frost days and ice days, rising zero degree line (Section 3.4.2)	Fewer and warmer cold days and nights and fewer frost and ice days (Section 4.3.3 and 4.3.4)	Very high	Circulation changes
Winter coldwaves / cold extremes	General decrease along with winter warming potentially amplified by snow albedo feedback and pronounced warming in source region of cold-air advection	Weakly decreasing frequency and duration (Section 3.4.2)	Decreasing frequency, intensity and duration but cold waves will continue to sporadically occur over coming decades (4.3.4)	High	Circulation changes (changes in winter blocking frequency and persistence) and potential effect of Artic amplification and sea-ice melt on midlatudinal weather
Heavy rainfall	More intense as a result of higher water carrying capacity of warmer air	Majority of stations with trends to more frequent and intense heavy rainfall events in all seasons (Section 3.4.3)	More intense and frequent heavy rainfall events in all seasons, in particularly in the cold season, the more intense the events the higher the increase (section 4.3.6)	Medium-high	Large-scale circulation changes, vertical stability and wind, small-scale convective processes
Dry spells / droughts	Increased probability of summer droughts and dry spells due to enhanced evapotranspiration, earlier snow melt and vegetation onset leading to soil drying and potentially more dry days	No robust and significant trend in summer mean precipitation and drought indicators (Section 3.4.3)	More frequent soil moisture droughts (soil moisture droughts) Tendency to more and longer dry spells (meteorological drought) (section 4.3.7)	Medium	Circulation changes (persistence of anticyclones, large-scale circulation changes), precipitation processes, strength of land-surface atmosphere interactions (soil moisture and vegetation feedbacks, convection, boundary layer processes)
Winter storms and extreme wind speeds	Intensification of cyclones due to latent heat release, changes in latitudinal temperature gradient affecting storm tracks	No robust trend but high decadal variability (Section 3.4.5)	No evidence for changes (4.3.8) changes cannot be ruled out	Low	Circulation changes (frequency, intensity and track of cyclones)
Hail	Not clear (Box 4.3)	No observational evidence for changes	No model evidence for changes (spatial scale too small)	Very low	Small-scale convective processes
Tornadoes	Sign not clear, competing effects of decreasing wind shear, and moistening / warming of boundary layer (Box 4.3)	Events of waterspouts and few tornadoes documented, no evidence for changes	No model evidence for changes (spatial scale too small)	Very low	Vertical wind shear, change in convective available potential energy, storm initiation
Intense snow fall events (lowlands)	Sign not clear, winter warming and precipitation increase are competing factors at low altitudes (Box 4.3)	No observational evidence for changes	No model evidence for changes	Low	Circulation changes (frequency and persistence of cross-Alpine flows)

* Level of scientific understanding: This is an index on a 5-step scale (very high, high, medium, low, and very low) designed to characterize the degree of scientific understanding. The index represents a subjective expert judgment about the reliability of the estimate, involving such factors as the significance of observed changes; uncertainties in how model capture the relevant mechanisms, agreement among different models, and theoretical process understanding.

Table 6.2. Synthesis table for different types of extremes. The projections and levels of uncertainty (LOSU) are valid for moderate- to high-emission scenarios and a mid- to end-of-century time period.